RESPONSE ANALYSIS OF SOFT SUBGRADE SUBJECTED TO MOVING LOAD

A DISSERTATION

SUBMITTED IN PARTIAL FULFILLMENT OF THE REQUIREMENTS FOR THE AWARD OF THE DEGREE
OF

MASTER OF TECHNOLOGY
IN
GEOTECHNICAL ENGINEERING

Submitted by:

Avneet Lahariya

(2K20/GTE/06)

Under the supervision of

Prof. Ashutosh Trivedi

DEPARTMENT OF CIVIL ENGINEERING
DELHI TECHNOLOGICAL UNIVERSITY
(Formerly Delhi College of Engineering)
Bawana Road, Delhi-110042

May, 2022

DELHI TECHNOLOGICAL UNIVERSITY
(Formerly Delhi College of Engineering)
Bawana Road, Delhi-110042

CANDIDATE'S DECLARATION

I, Avneet Lahariya, Roll No. 2K20/GTE/06, student of M.Tech (Geotechnical Engineering), hereby declare that the project dissertation entitled "Response Analysis Of Soft Subgrade Subjected To Moving Load" which is submitted by me to the Department of Civil Engineering, Delhi Technological University, Delhi in partial fulfillment of the requirement for the award of the degree of Master of Technology, is original and not copied from any source without proper citation. This work has not previously formed the basis for the award of any Degree, Diploma Associateship, Fellowship or other similar title or recognition. Responsibility of any plagiarism issue stands solely with me.

Place: Delhi (**AVNEET LAHARIYA)**

Date: May 31, 2022

DEPARTMENT OF CIVIL ENGINEERING
DELHI TECHNOLOGICAL UNIVERSITY
(Formerly Delhi College of Engineering)
Bawana Road, Delhi-110042

CERTIFICATE

I hereby certify that the Project Dissertation entitled "**Response Analysis Of Soft Subgrade Subjected To Moving Load**" which is submitted by Avneet Lahariya, Roll No. 2K20/GTE/06, to Department of Civil Engineering, Delhi Technological University, Delhi in partial fulfillment of the requirement for the award of the degree of Master of Technology, is a record of the project work carried out by him under my supervision. To the best of my knowledge this work has not been submitted in part or full for any Degree or Diploma to this University or elsewhere.

Place: Delhi
Date: May 31, 2022

(ASHUTOSH TRIVEDI)
PROFESSOR & SUPERVISOR
Department Of Civil Engineering

ABSTRACT

The transportation network on soft subgrade is an active interest among researchers due to the rapid urbanization of human civilizations. The soft subgrade is stabilized using geosynthetic to prevent undesired deformations and failure. In the present study, a numerical model is developed to examine the dynamic response of unpaved road using commercialized finite element software Abaqus. The dynamic implicit method is adopted to evaluate the velocity-induced load-deformation response of the soft subgrade. The numerically obtained results for unreinforced roads are compared with geosynthetic reinforced roads. The study showed that geosynthetic reinforcement improves serviceability under moving vehicle load by reducing and uniformly distributing vertical stresses on the subgrade. The maximum displacement of the subgrade layer is reduced to 74% by stabilizing with the geosynthetic material. The results demonstrate that the displacement response is increased with the increase in loading intensity. The introduction of geosynthetic reinforcement improves the threshold velocity (from 20 m/s to 27 m/s) of moving load on unpaved road supported by the subgrade layer. The study shows that geosynthetic reinforcement can be a viable solution to subsurface improvement for a shorter maintenance cycle, particularly on weak sub-grade.

ACKNOWLEDGEMENT

I, Avneet Lahariya (2K20/GTE/06) would like to express my sincere gratitude to Hon'ble Vice-Chancellor, Head of Department, faculties of Geotechnical Engineering, lab staff and friends for supporting me throughout the project. It is indeed a great pleasure and privilege to present this report of Major Project-2 entitled "Response Analysis of Soft Subgrade Subjected to Moving Load" under the guidance and supervision of Prof. Ashutosh Trivedi Sir.

I would personally like to thank Prof. Ashutosh Trivedi Sir for his patience, insightful comments, practical advice and motivation which helped me tremendously in the project work. Without his guidance and support, this project would have not been completed.

Additionally, I would like to express gratitude to Mr. Yakshansh Kumar and Mr. Kshitij Gaur for their treasured support which was really influential in shaping my numerical simulation and technical guidance.

I also express my deep gratitude to the Department of Civil Engineering and all the faculty members of Civil Engineering Department, Delhi Technological University, Delhi for the kind support in the progress of my research work. Last but not the least, I would like to thank my family who inspired and motivated me for the successful completion of my dissertation work.

(AVNEET LAHARIYA)

Roll No. - 2K20/GTE/06

CONTENTS

LIST OF TABLES

LIST OF FIGURES

LIST OF SYMBOLS, ABBREVIATIONS

C	=	Damping coefficient
CPT	=	Cone Penetration Test
C$\dot{x}$	=	Losses in the system
DCPI	=	Dynamic Cone Penetration Index
DCPT	=	Dynamic Cone Penetration Test
F	=	External applied load
K	=	Spring constant
K*x*	=	Stiffness of the material
M	=	Mass of the system
M-S-D	=	Mass Spring Damper
M$\ddot{x}$	=	inertial component
v	=	Velocity of moving load

CHAPTER 1
INTRODUCTION

The following chapter will help understand the response of soft sub-grade, which is stabilized by reinforcing with the geosynthetic material. A numerical program has been adopted to analyze the behavior of soft sub-grade. The parameters will be calculated at the different magnitudes of moving loads and velocities based on the data obtained from past studies.

1.1 General

Due to rapid urbanization, the transportation network is constructed on marginal and low-strength soil (soft soils). The heavy-moving vehicles can cause undesired ruts, and excessive deformation on the road surfaces often results in frequent maintenance and reduced stability. The viable solution to prevent the failure of the road surfaces is by stabilizing them with reinforcement. Geosynthetic layers as reinforcement are frequently used to improve the poor/weak soil subgrade for paved and unpaved roadways.

The use of geosynthetic as a reinforcement material in paved and unpaved road construction dates back to the 1970s. Many experimental and computational studies have been published since then to understand the benefits of employing geosynthetics in road construction. Several researches have shown that geosynthetics used to reinforce unpaved roads on soft ground can provide better confinement for the material, reduce rut depth, increase load bearing capacity, lengthen service life, and minimize the amount of fill required.

The main objective is to study the behaviour of soft subgrade under moving loading conditions and establish relationships between different loading intensity with variable velocities. In the present study, an attempt has been made to obtain a numerical model of unpaved road system using finite element software Abaqus. The model consists 3 layers of soil material named as base course, sub-base course and soft subgrade. The subgrade has been modelled using the Mohr's coulomb constitutive model. The dynamic implicit program has been adopted to simulate the behaviour of soft subgrade dynamically. The loading has been applied by using Dload subroutine code in which variable loading intensity of vehicle are changes with variable velocities. The 8-node 3D stress linear brick element has been used for meshing the model and reduced

integration scheme is adopted for analysis. The displacement response has been recorded at variable vehicular velocities and load intensities. The results are then compared among unreinforced and reinforced unpaved road. The efficiency of the geogrid has also been evaluated with variation of vehicular velocities. This will help geotechnical engineer to know behaviour of soft subgrade soil under the moving load.

1.2 OBJECTIVES OF THE STUDY

The project deals with the following objectives:

- To evaluate the response of soft subgrade under moving load.
- To establish the relationship curve for the velocity-induced load-deformation characteristics.
- To estimate the efficiency of reinforcement after stabilisation of unpaved road.

1.3 ORGANISATION OF CHAPTERS

The following chapters have been incorporated in this project report:

In chapter 1, the project title has been introduced in detail. The main objectives and outlines of the work have been discussed.

In chapter 2, the study of the research papers and their findings are mentioned. After following various research papers and books, research gaps has been founded and mentioned.

In chapter 3, the materials used in this project and the methodology followed have been described.

In chapter 4, the results obtained in this project have been listed and discussed in detail.

In chapter 5, the conclusions have been summarized and the recommendations for future work are mentioned.

CHAPTER 2

LITERATURE REVIEW

2.1 INTRODUCTION

From over 2,000 years ago, road builders used bamboo, straw, small bushes, tree trunks, and stones to stabilize roads. The concept of geosynthetics has been developing in recent years. By 1980, the use of geosynthetics, or as it was referred back then "geotechnical fabrics" was gaining more popularity throughout the road construction industry. However, uncertain design criteria and limited performance history were major limitations. Nowadays, the utilization of geosynthetics is limited to standard axle load only as there is no study present to check the compatibility of these with heavy axle load.

2.2 LITERATURE REVIEW

The analysis of unpaved roads subjected to the dynamic loads is motivated by practical and on-site conditions. The basic idea of the present approach of static loading should be known to understand the effect of these loading conditions. Various researchers gave fundamental theories and suggestions based on the test results obtained on unpaved roads. The recent research includes testing unpaved roads with and without geosynthetics subjected to standard legal loading conditions, which are as follows.

- According to Keller (2016), there are alot of applications of geosynthetics on low-volume road which are under-utilized. Significant cost saving and design improvement can be obtain using geosynthetics. The study provided by Peketi (2019), shows that the utilization of geogrids in flexible pavement can effectively reduce the pavement thickness upto 40% without compromising the strength.
- As stated by Theuns et al (2006) that failure in roads are classified as surface and structural defects. Surface defects such as corrugations, roughness, rutting, potholes, erosion, loss of surface material, ravelling, and slippery surface mainly affect ride quality. The failure of the sub-grade or pavement layers results in structural defects. Patches on the surface, more significant depressions or loss of pavement are symptoms of structural defects. The pavement depth, material used, road geometry, and poor drainage are the major causes of structural defects.

- When gravel surface deteriorates, change in gravel surface thickness over time. It will result in surface roughness, undulation, and rutting, as shown by Kuleno and Lera (2020).
- Geotextile and geogrid reinforcement proved to be the most effective reinforcement, and the contribution of geomat was least in improving the performance of the subgrade-aggregate composite system. The reinforced subgrade-aggregate composite system performs better than the unreinforced subgrade-aggregate composite system. It is observed in the case of geotextile and geogrid reinforcement placed at the subgrade and aggregate layer interface.
- The contribution of reinforcement by geosynthetics will be ineffective if placed at an unsuitable location.
- The result of the dynamic cone penetration test (DCPT) shows that the dynamic cone penetration index (DCPI) value decreases for the reinforced test section compared to the unreinforced test section due to the inclusion of geotextile and geogrid. The lowest DCPI value is obtained for the geotextile-reinforced test section. Greater penetration resistance is observed for the geosynthetic reinforced test section compared to the unreinforced test section, as followed by Singh et al (2020).
- Various materials have been utilised for reinforcement and stabilisation purposes in soil. Stabilisation with fly ash is often used. The static cone penetration test (SCPT) results analysed by Trivedi and Singh (2004) at various combinations of stress level and relative density indicated the need for a new scheme to interpret the behaviour of ash fills based on the relative dilatancy of the ash. Therefore, relative dilatancy plays a significant role in analysing stress distribution.
- It is necessary to scientifically carry out a soil survey and test the representative samples for standard IS classification tests, compaction tests and California bearing ratio (CBR). The depth of ground water table (GWT) and its fluctuations, annual rainfall, and other environmental conditions that influence the due subgrade strength must be investigated. (IRC SP: 72).
- A classical literature has been written by Zafir (1994), Mamlouk (1997), and Hardy (1993) and Cebon (1994) on the problems caused due to moving load on pavement response. A basic generalised equation of motion for the solution of moving load on

the pavement under various conditions using the D`Allembert principle can be given as:

$$M\ddot{x} + C\dot{x} + Kx = F \quad (1)$$

- where, m, c, and k are mass, damper, and stiffness matrix and $\ddot{x}$, $\dot{x}$, x and F are acceleration, velocity, displacement, and force vector respectively.

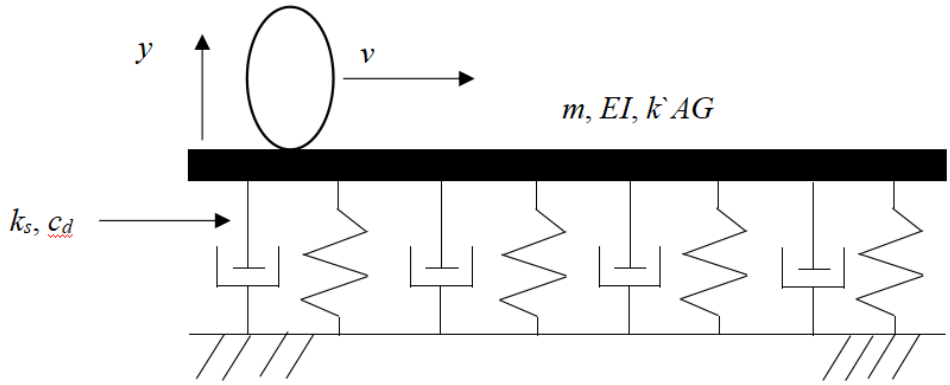

Figure 2.1 An infinite beam on viscoelastic foundation subjected to moving load (Chen and Huang, 2000)

- Here, k_A and I represent the effective shear area, and the second moment of area of the beam section E and G represent the Young's and shear moduli of the beam; k_s and c_d represent the coefficient of the foundation stiffness and viscous damping per unit length of the beam.
- General analytic solutions to the problem of the response of elastic beams and plates supported on the elastic foundation and elastic half-plane or half-space media to moving loads of constant or variable speed were reviewed by Fryba (1987; 1999).
- The pavement modelling is done by idealising the pavement as a beam by Chen and Huang (2000) and plates by Sun and Luo (2007) on the elastic damped foundation of the Winkler type subjected to moving load.
- Now, considering moving load on the unpaved road system, material behaviour is viewed as linear elastic for the beam or plate (simulating the pavement) and the foundation springs or the half-plane (space) (simulating the supporting soil). The supporting soil may also have viscous dampers along with the springs or exhibit linear viscoelastic behaviour, as discussed by Cao et al. (2010) and Tang et al (2020).
- The analysis of pavement is generally done by assuming it to be a plate resting on the soil medium or as an elastic beam. The dynamic analysis is done by considering

the unpaved roads as linear elastic material.While in reality, the use of flow-controlled material in the analysis should be done as observed by Mehra and Trivedi (2021).

- In the mathematical analysis, different models were proposed to analyse the behaviour of unpaved roads based on different vehicle speed, loading, and pavement material. The finite element method was applied in the numerical simulation, to estimate the deformations, strains, and stress levels in the system.

2.3 RESEARCH GAP

By going through various research papers, textbooks and codal provisions, the following research gaps came under light:

1. There is no relationship curve between the velocity-induced load-deformation curves for the unpaved road stabilised using geosynthetics. In this study, a relationship curve has been given before and after the reinforcement of subgrade.
2. The threshold velocity for soft subgrade at which the amplification of displacement changes with the load and velocity.
3. Meagre work has been on vibratory load caused by vehicular movement.

CHAPTER 3

MATERIALS & METHODS

3.1 NUMERICAL METHOD

FEM is a numerical method which provides approximate solutions to field problems. Mathematically speaking, field problems are expressed by partial differential equations for which the solution also satisfies the boundary condition, i.e. boundary value problems (BVP). However, finite element analysis (FEA) aims at only approximating the field quantity with a piecewise interpolation. Therefore, the approach of using the finite element method should be adopted to simulate the behaviour of unpaved road systems. The numerical analysis has been performed by using Abaqus software.

3.2 MODELING ASSEMBLY

A unpaved road model consisting of 3 layer of soil material has been developed. The layers of soil material are as:- base course, sub-base course and soft subgrade. The placement of these soil layers is shown in the Figure.2. Initially, the soft subgrade is modelled which is followed by the sub-base course and then base course layer. The dimension of the soil layers are given in Table 1. The thickness of the base course, sub-base course and soft subgrade layers are 150, 200 and 500 mm respectively which has been considered from the IRC-37 (2018) – "Guidelines for design of the flexible pavement".

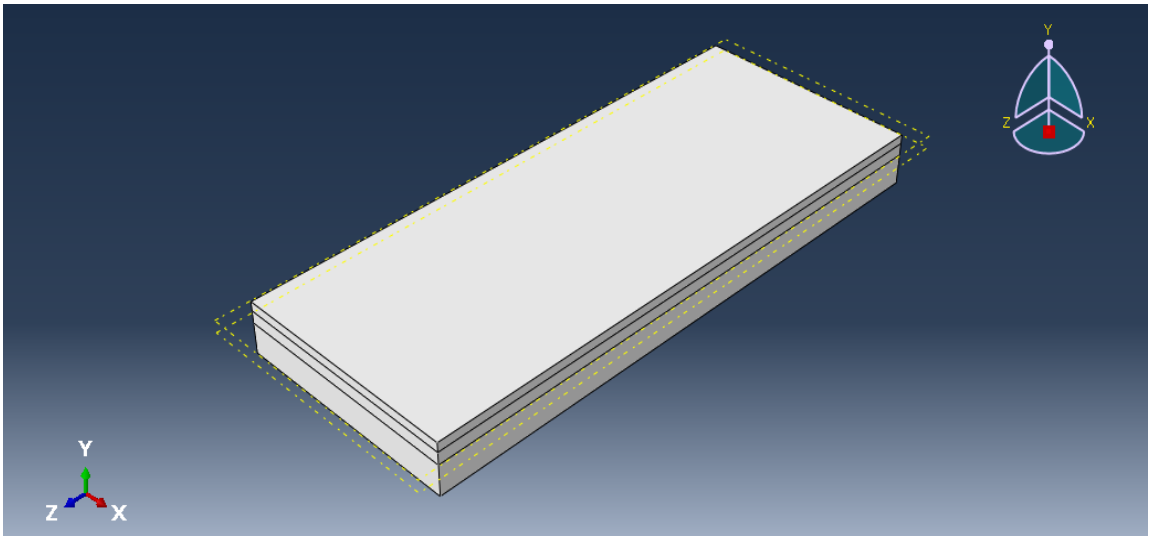

Figure 2: Model of the unpaved road

Table 1: Dimension of the layers

S.No.	Soil layer	Length (m)	Width (m)	Thickness (m)
1.	Base course	10	4	0.15
2.	Sub-base course	10	4	0.2
3.	Soft subgrade	10	4	0.5

3.3 MATERIAL PROPERTIES

In this study, the unpaved road model consists of 3 soil layers having different material properties. These layers are the base course, sub-base course and subgrade layer.

Base course layer – It is the uppermost layer of the unpaved road model. As per the IRC-37(2015), the layer consists of wet mix macadam (WMM), water-bound macadam (WBM), crusher run macadam etc. Still, among these materials, the unbound soil material or sand has been considered. The base course layer has been modelled as an elastic material. The void ratio of 0.45 has been considered for sub-base layer.

Sub-base course layer – It is modelled as the middle layer of the road model, which generally serves three functions which are as follows:- (1) provide support for the compaction of the base layer, (2) protect the subgrade layer from overstressing, (3) for drainage purposes. The sub-base layer is generally considered a granular layer which is unbound and bounded with the cement, fly ash and other chemical stabilizers. In this study, the layer consists of crushed stone mixed with gravel soil modelled as an elastic material. The void ratio of 0.35 has been considered for sub-base layer.

Subgrade layer – The subgrade is the bottom layer of any road, consisting of in-situ natural soil material. The function of the layer is to distribute the vehicular moving load inside the earth's surface. In this study, the subgrade layer is considered a soft soil or clayey soil having meagre shear strength, which can show undesired ruts and excessive deformations on the surface, causing the failure of the unpaved road. The soft subgrade is considered a constitutive model of Mohr-Coulomb plasticity as a cohesive soil with cohesion yield strength of 8 kPa with negligible frictional strength (Chawla and Shahu, 2021). For numerical stability of the algorithm in the software, the soil's friction angle and dilation angle are considered as 1° and 0.85°, respectively (Satyal et al. 2018). The

void ratio of the subgrade layer has been taken as 0.9. The subgrade layer can be stabilized by reinforcement techniques using geosynthetic materials.

Geosynthetic layer – Geosynthetic materials are usually made of the polymer compound (hydrocarbon). They are used with soil or rock in road and track construction to strengthen weak soil. Geotextiles, geogrids, geonets, geomembranes, geocomposites etc., are the different types of geosynthetic materials. This study has embedded a two-layer of geogrid in the unpaved road model. One layer is at the interface of the base course & sub-base course, and another layer is at the interface of the sub-base & subgrade. The thickness of the geogrid layer has been taken as 5 mm.

Table 2 shows the material properties of all layers of road and geogrid which is as given below:

Table 2: Material properties

S. No.	Components	Density (Kg/m^2)	Elasticity (MPa)	Poisson ratio
1.	Base course	2160	55	0.35
2.	Sub-base course	1920	25	0.35
3.	Soft subgrade	1830	1.25	0.4
4.	Geogrid layer	930	2625	0.2

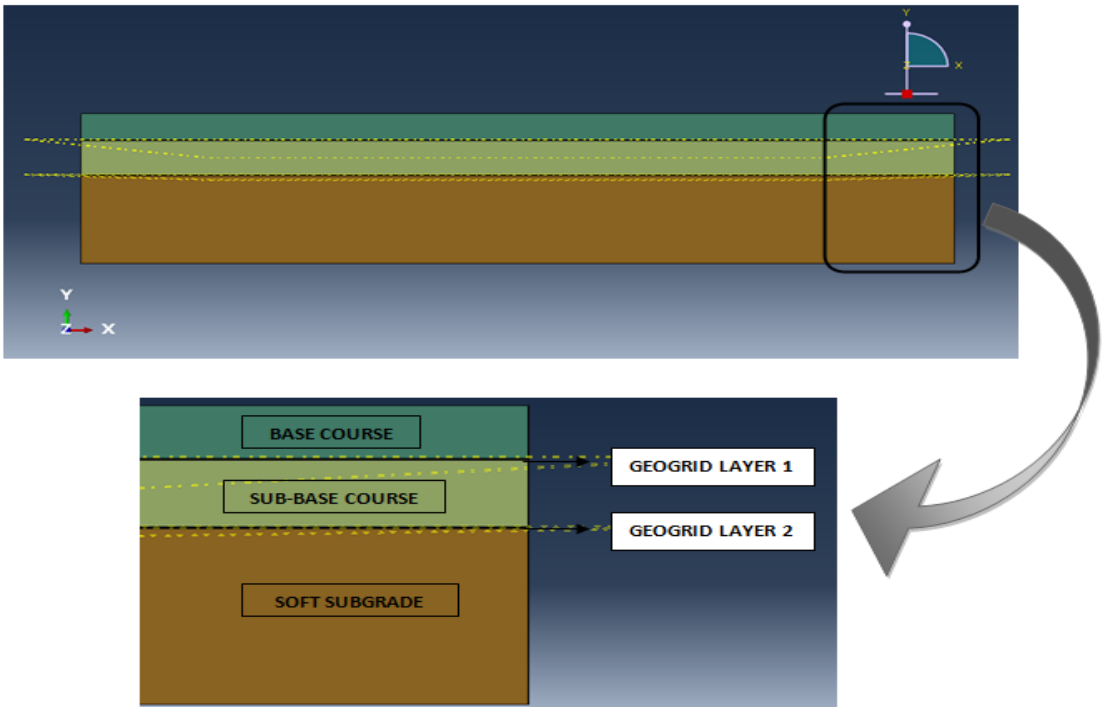

Figure 3: Location of geogrid in the model

3.4 LOADING MODULE

3.4.1 Load application

As per IRC-58 (2015), the allowable load limits of variable axle of vehicle which are subjected to roads are given in Table 3. The loads are moving with variable velocities that are ranges from 10 to 30 m/s with the increment in velocity of 5 m/s.

Table 3: Load intensity of moving vehicle on the basis of axle configuration

Axle configuration	Magnitude of Load (kN)
Single axle single wheel	68
Single axle dual wheel	100
Tandem axle	186
Tridem axle	235

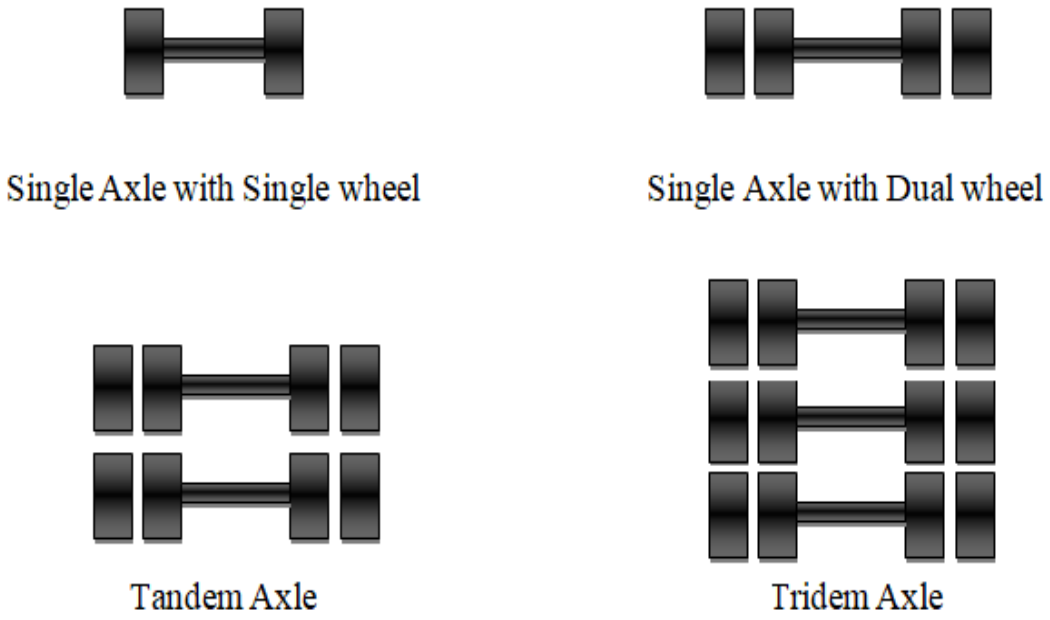

Figure 4: Axle configuration of the load

The load is applied on the road with the help of Dload subroutine. A subroutine is a coded file (developed using FORTRAN programming language) which has been used to define the variation of magnitude of distributed load as a function of position of co-ordinates, time, element number, etc. Considering the all axle configuration of load, the single patch of rectangular area is coded in the subroutine file which signifies the tire contact area with the surface of road. The top view of the tire imprintation with the

surface of road is shown below in the Figure 5 and the subroutine file interface is shown below in the Figure 6

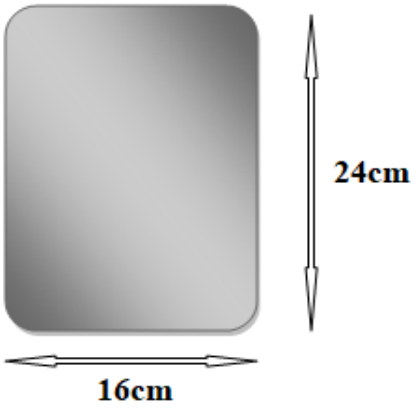

Figure 5: Dimensions of the tire imprint on the surface of road layer

```
      subroutine DLOAD(F,KSTEP,KINC,TIME,NOEL,NPT,LAYER,KSPT,
     &                 COORDS,JLTYP,SNAME)
C
      include 'ABA_PARAM.INC'
C
      dimension TIME(2), COORDS(3)
      CHARACTER*80 SNAME

      X=COORDS(1)
      Y=COORDS(2)
      Z=COORDS(3)

      Velocity = 10.0
      Z_position = Velocity*TIME(1)

      if (Z.le.(Z_position+0.12).and.Z.ge.(Z_position-0.12).and.X.le.0.08
     &     .and.X.ge.-0.08)then
         F = 68000.0
      else
         F = 0.0
      endif

      RETURN
      END
```

Figure 6: Subroutine coded file for velocity and load application

3.4.2 Boundary conditions

The boundary conditions in Abaqus are used to specify the basic value of variables like velocity, displacement, rotation, etc at nodes of the model. It can also be used to restrict the motion of boundary faces. In this study, the encastre boundary condition has been considered to restrict the every type motion of soil at the faces of XY and YZ plane (all the vertical faces of the model) when it is subjected to moving load.

Encastre boundary condition – The nodes situated at faces have 0 degree of freedom that is:-

Translational movement: - U_1, U_2, $U_3 = 0$

Rotational movement: - UR_1, UR_2, $UR_3 = 0$

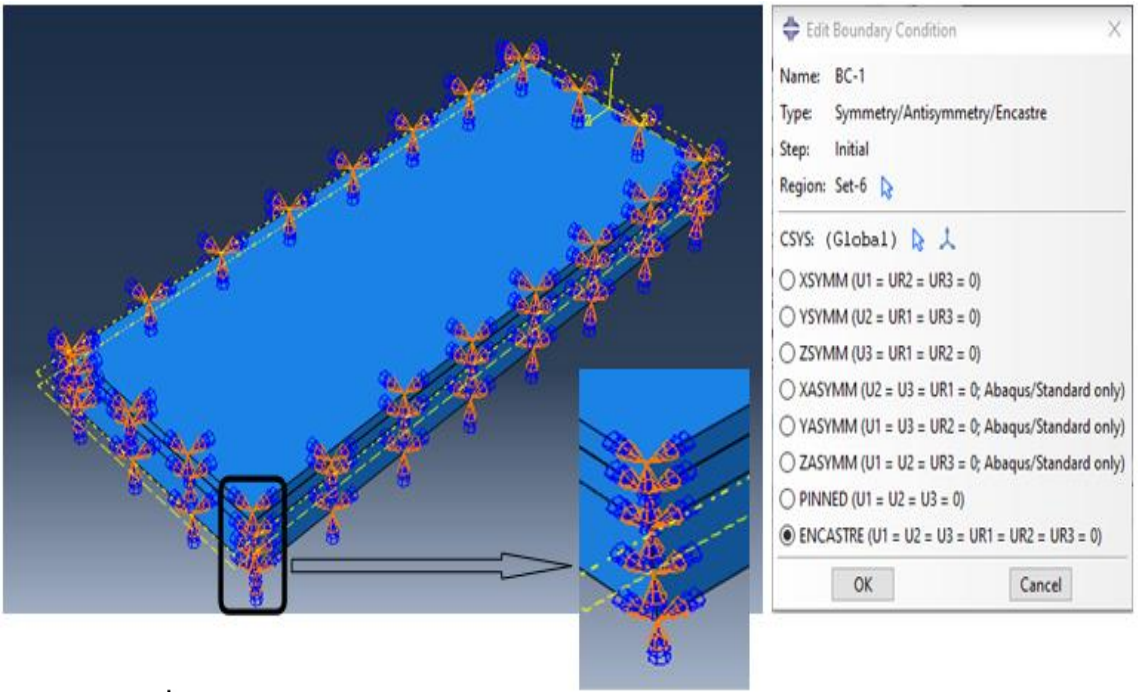

Figure 7: Boundary condition on the model

The M-S-D model has been considered for the bottom of subgrade layer as the soil is infinite in the lower direction. The spring coefficient (k) and dashpot coefficient (c) value has been taken for making the model as the spring dashpot. The MSD model has shown in the Figure 8

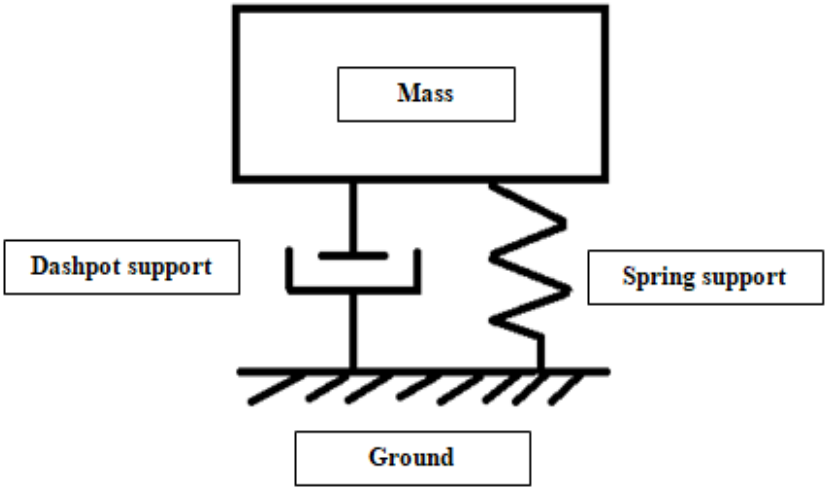

Figure 8: M-S-D model of the system

The value of the spring constant has been taken as 2.71×10^7. The damping ratio (ζ) of the soil has been taken as 5% (ranges from 0 to 20%) (Wu and Shen, 1996). The dashpot coefficient calculation is shown below:-

$$\zeta = \frac{C}{C_m} \quad (2)$$

$$C = \zeta . C_m \quad (3)$$

Where :- C = Dashpot Coefficient

C_m = Critical dashpot coefficient

$$C_m = 2\sqrt{km} \quad (4)$$

Table 4 Calculation of mass of the model

Components	Density (kg/m^3)	Volume (m^3)	Mass (kg)
Base course	2160	6	12960
Sub-base course	1920	8	15360
Soft subgrade	1830	20	36600
	Total mass		64920

Thus, the damping coefficient can be calculated by putting all the values in eq. (3), which comes out of 132.640 kN-s/m.

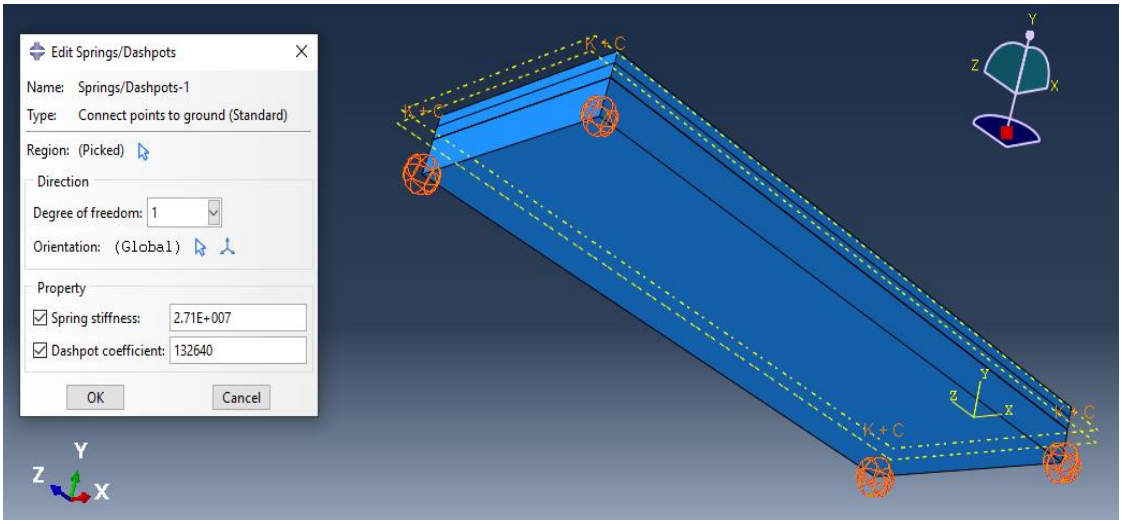

Figure 9: Application of spring dashpot coefficient in the subgrade layer

3.5 INTERACTION MODULE

The interaction is referred to as the contact between the model layers. The interface condition in a multi-layer pavement system has a significant impact on-road performance. The general contact interaction can be used to define property for the surfaces by using single interaction. It has been used to interact the subsequent road layers, with "hard" normal contact, and for tangential contact, the friction coefficient has been taken as 0.3.

3.6 MESHING OF THE MODEL

Meshing of the model refers to break down the parts of model into the number of element. These parts of the model can be mesh in two ways: - local or global level. The variety of mesh control is:-

(1) Element shape

(2) Meshing technique

(3) Meshing algorithm

(4) Adaptive remeshing rule

The model incorporates biased meshing to concentrate finer elements beneath the load and pavement interface. A C3D8R element which refers as 3D plane stress reduced – integration brick element has been used to mesh the layers of unpaved road.

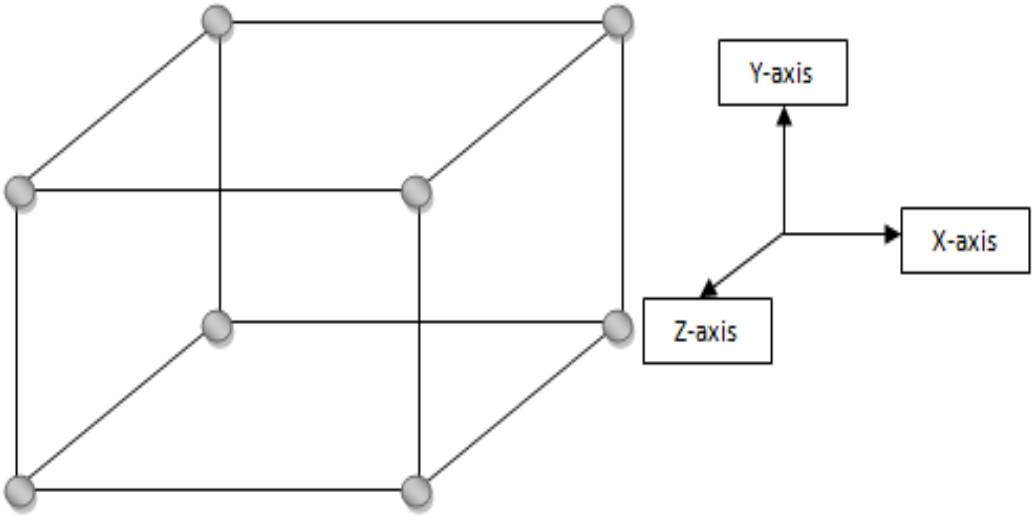

Figure 10: C3D8R element (3D plane stress reduced-integration brick element)

Elements for the base course layer have an average size of 15 mm to indicate the size of the base course. Mesh sensitivity tests were performed on the model, and the meshes used shown acceptable accuracy when compared to meshes with more components.

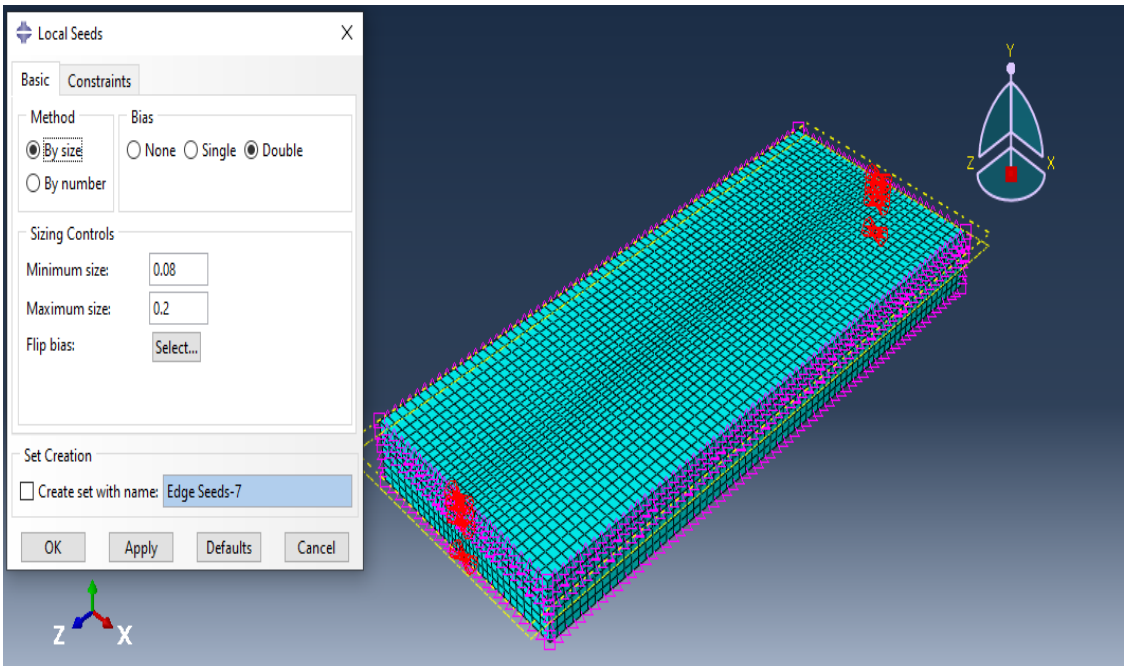

Figure 11: Meshing of the model

3.7 STEP MODULE

Dynamic implicit scheme has been used to simulate the model which consist direct integration dynamic analysis for non linear behaviour of material. It can be used to study variety of application such as:-

- dynamic response involving transient fidelity and low energy losses;
- dynamic responses involving contact, nonlinearity, and moderate energy dissipation;
- quasi-static responses with significant energy dissipation provide stability and enhanced convergence behaviour for identifying an effectively static solution.

The time-dependent direct integration approach has been used to capture the impacts of moving vehicle loads. The displacement has captured using the D'Allembert principle, and the motion equation is given by

$$M\ddot{x} + C\dot{x} + Kx = F \qquad \textbf{5}$$

Where:-

M = mass of the system

C = damping coefficient

K = spring constant

F = external applied load

In this equation, the $M\ddot{x}$ denotes the inertial component; $C\dot{x}$ denotes the losses associated with the system and Kx denotes the stiffness of the material. F denotes the external forces applied on the MSD system which can be constant, vibration load with variable frequency, impact load etc.

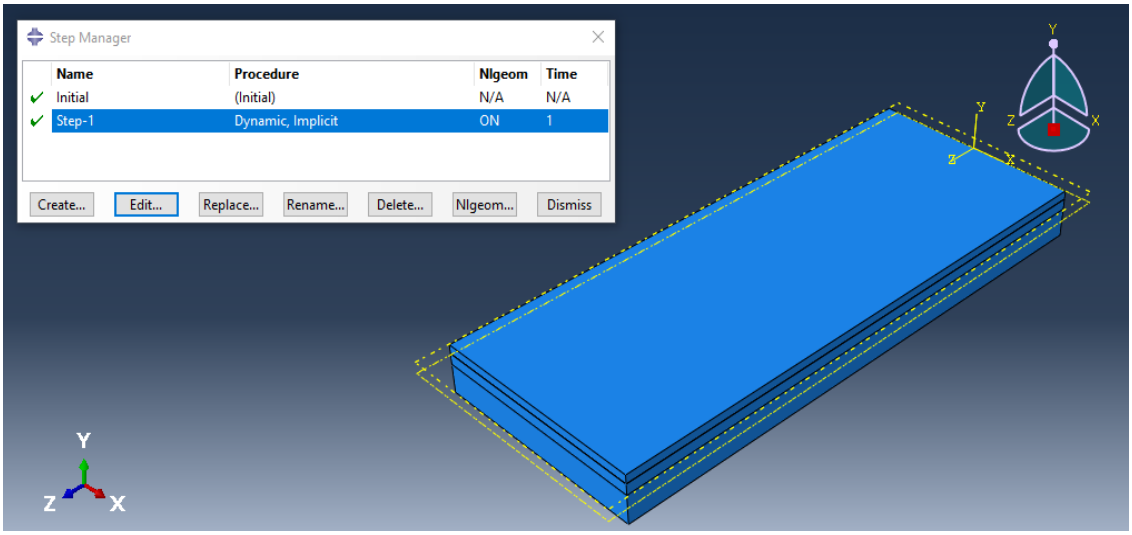

Figure 12: Application of dynamic implicit property of the model

CHAPTER 4

RESULTS AND DISCUSSION

4.1 RESULTS

The results of present model have been validated with the experiential findings of Singh et al., (2021). Figure 13 shows the variation of vertical deflection of the subgrade layer along the width of subgrade for numerical and experimental investigations. The deflection of ruts on the subgrade has increased with increase in the cycles or the loading intensity of vehicle.

The central deflection at SASW load has been seen approximately at 1.2 mm with 10 m/s vehicular velocity in the present study which has been deviating from 1.3 mm as per the experimental study.

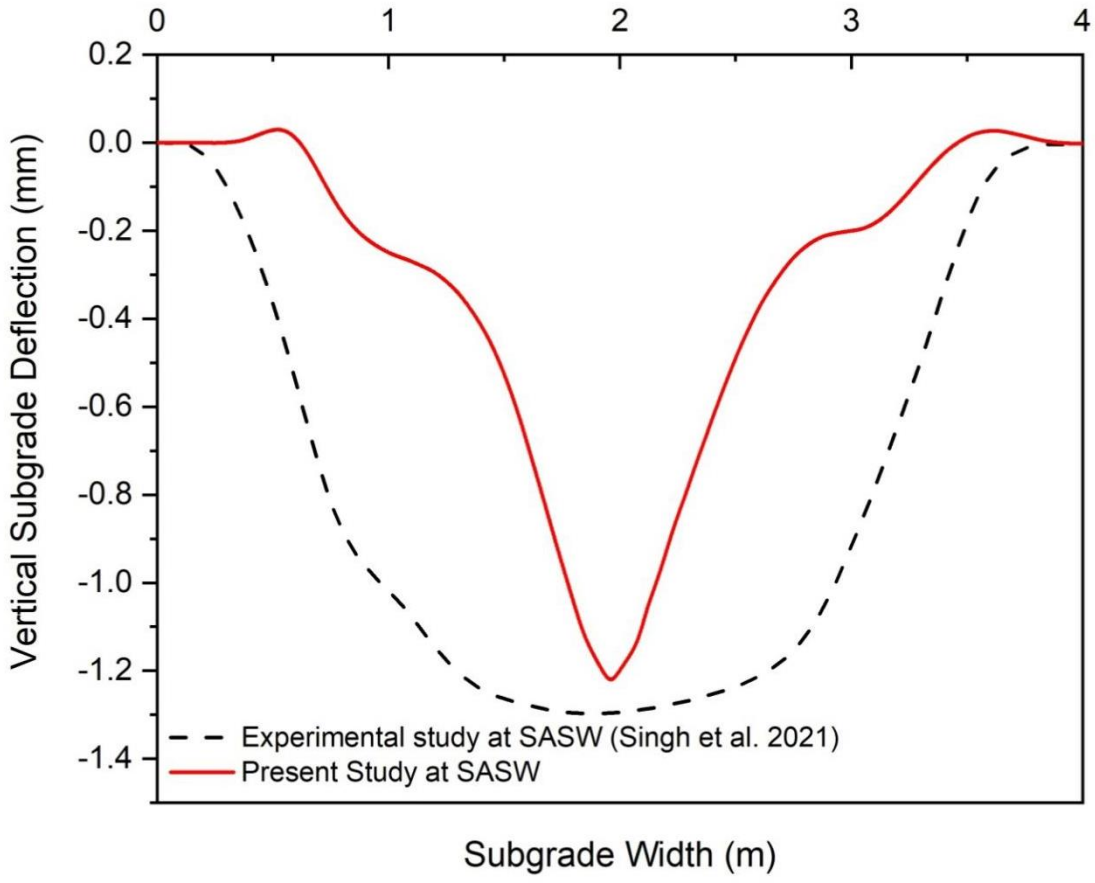

Figure 13: Vertical deformation of subgrade

All the results are calculated on the reference point which has been taken at the mid length of the subgrade that is 5 m from the starting point. The reference point is shown in the given Figure 14

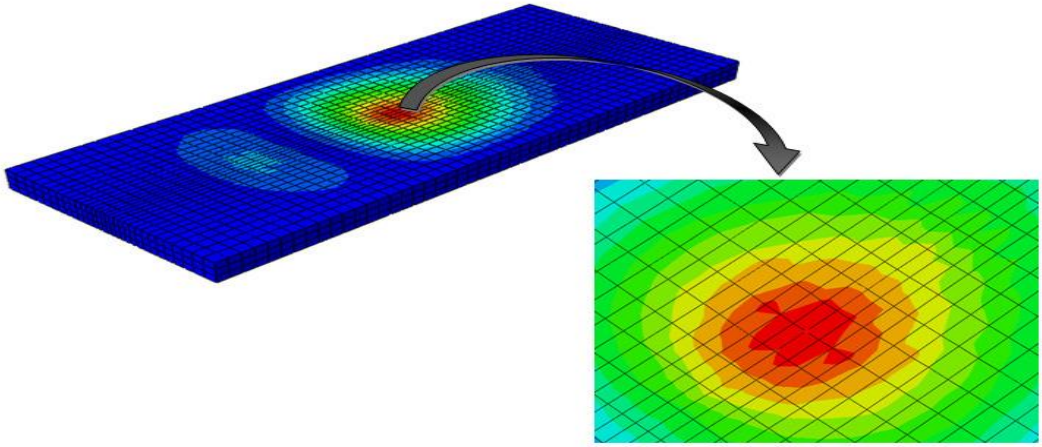

Figure 14: Reference node on the subgrade

Initially, the response of subgrade is calculated without reinforcing it with the geogrid layer. The deflection on the reference point has been noted for variable velocity of vehicle that is at the 10, 15, 20, 25, and 30 m/s and variable loading intensity of 68, 100, 186, and 235 kN.

The displacement contour showed the behavior of moving load on the soft subgrade which has been shown in the Figure 15

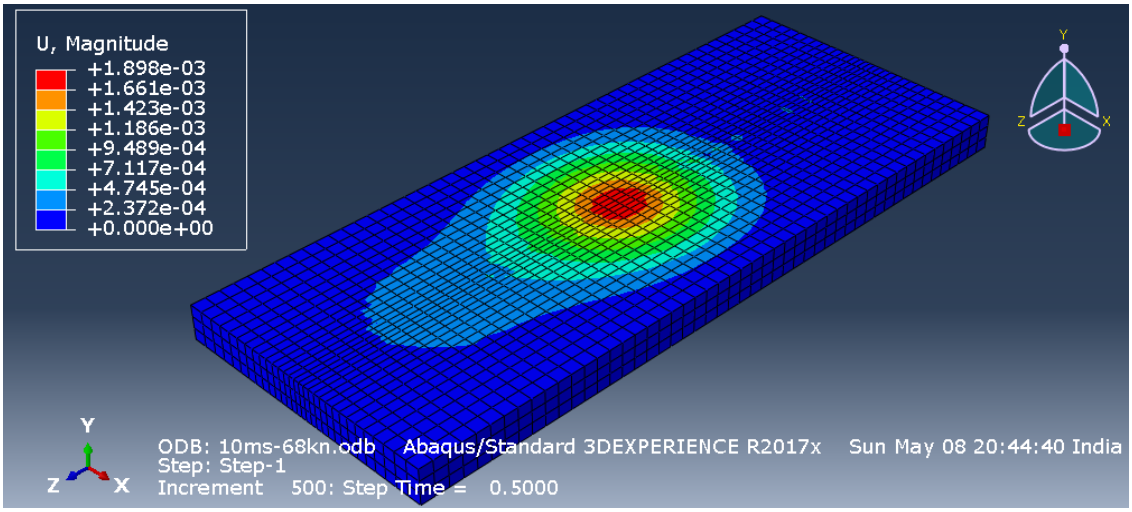

Figure 15: Displacement contour of the subgrade

The displacement response of soft subgrade in the vertical direction at the velocity of 10 m/s has been shown in the Figure 16 (a). The minimum and maximum deflection that has been noted are of 1.9 and 6.83 mm at the vehicular load of 68 and 235 kN respectively. The deflection has been seen to be increasing as the load approaches to the middle of the road layer and showed the peak values. Further, the deflection starts to decreases when the load passes the mid reference point of the road.

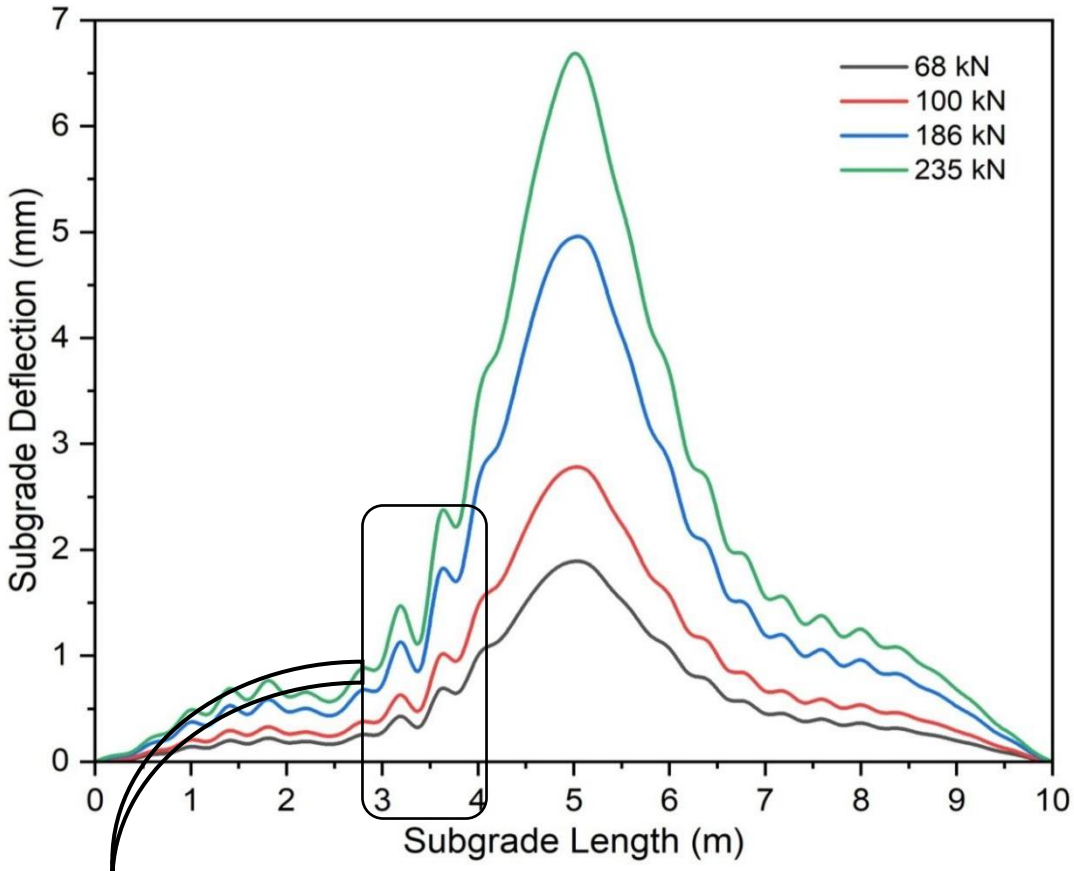

Figure 16(a)

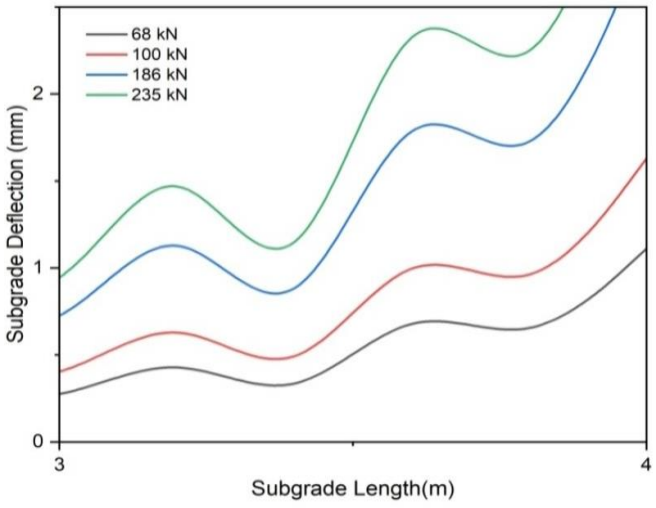

Figure 16(b)

Figure 16: (a) Response of unreinforced subgrade deflection at 10 m/s **(b)** Disturbance of unreinforced subgrade deflection at 10 m/s (enlarged between 3 m-4 m)

The disturbances that can be seen in the fig 16(a) (enlarged picture as shown in Figure 16(b)) are due to the boundary reflections and the vertical vibration caused by the moving vehicular load.. When the load moves on the surface of road, it will induce waves in all direction which reflects to the boundary layers of the model and distributed in the entire layer.

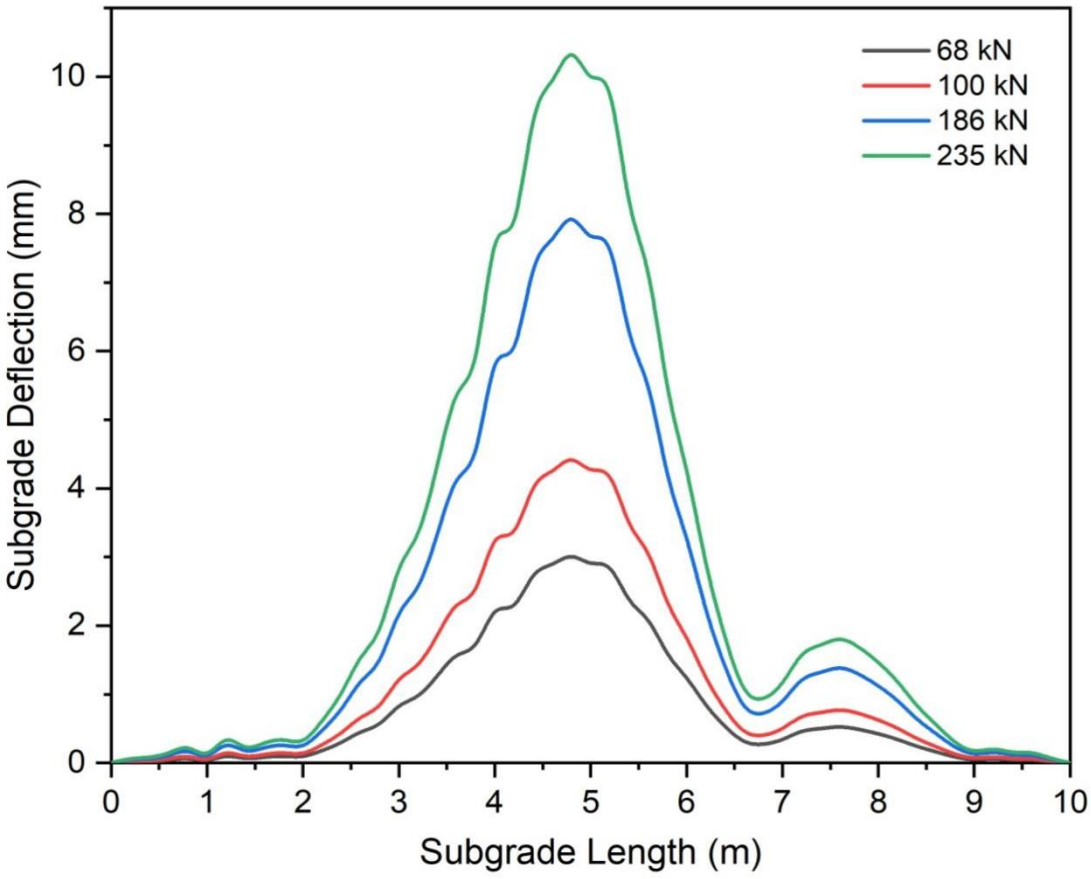

Figure 17: Response of unreinforced subgrade deflection at 15 m/s

Figure 17 shows the subgrade displacement response at vehicular velocity of 15 m/s. The minimum and maximum deflection that has been noted are of 3.07 and 10.55 mm at the vehicular load of 68 and 235 kN. The peak value of the all the curves can be seen at the middle length of the pavement that is at 5 m.

Figure 18 shows the subgrade displacement response at vehicular velocity of 20 m/s. The minimum and maximum deflection that has been noted are of 3.03 and 10.44 mm at the vehicular load of 68 and 235 kN. The maximum and minimum values of deflection at vehicular velocity at 20 m/s are slightly less than the deflection values at vehicular velocity at 15 m/s. The peak values of the curve also shifted to the left side of the middle length of subgrade and showed the peak values before 5 m of subgrade length (at 4.4 m of subgrade length). It has been shown due the interaction time of the load and

layers of the road. It also shows that when the load is at the 5 m of subgrade length, the deflection will not be maximum at that point with comparing to the results of vehicular velocity of 10 and 15 m/s.

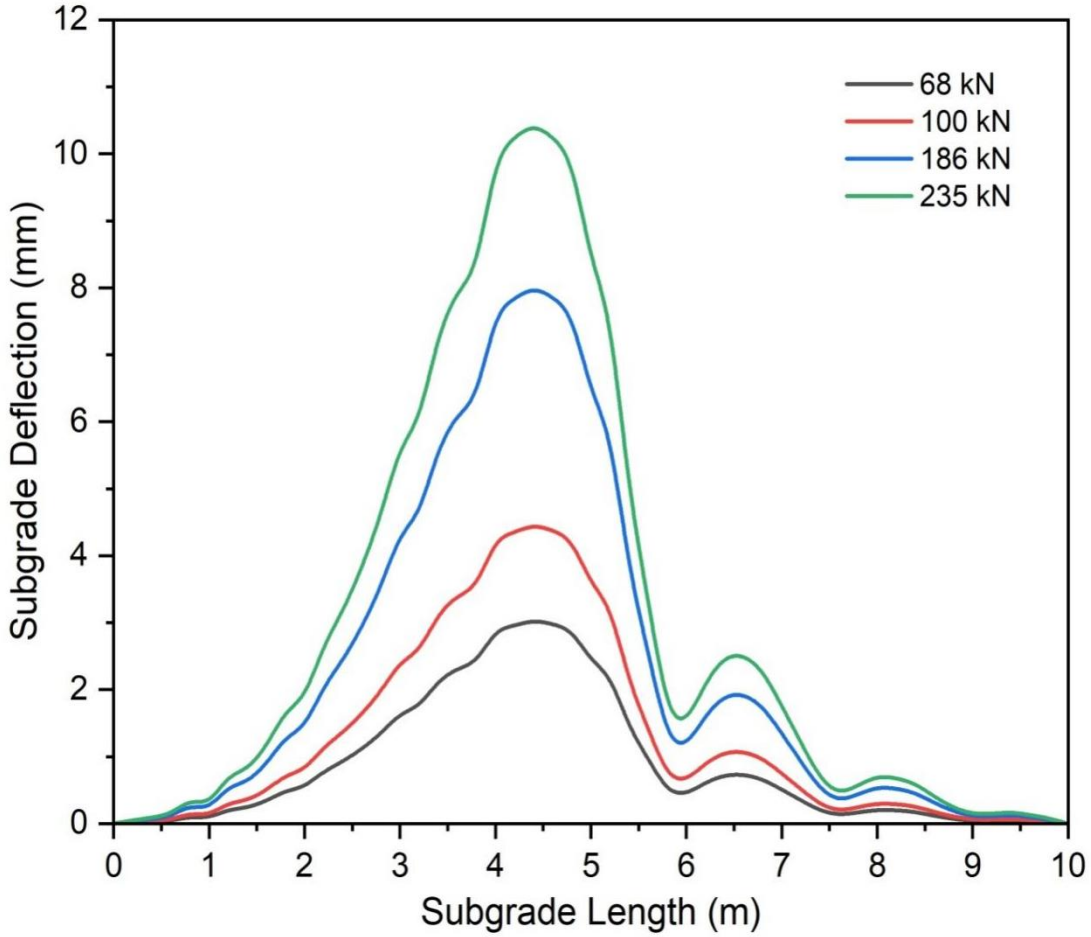

Figure 18: Response of unreinforced subgrade deflection at 20 m/s

Figure 19 shows the subgrade displacement response at vehicular velocity of 25 m/s. The minimum and maximum deflection that has been noted are of 2.7 and 9.3 mm at the vehicular load of 68 and 235 kN. The peak of deflection curve has been shifted more on the left side as compare to the previous results and peak values can be seen at 4 m of the subgrade length. The maximum value of subgrade deflection has also been reduced more from the previous velocity curve.

Figure 20 shows the subgrade displacement response at vehicular velocity of 30 m/s. The minimum and maximum deflection that has been noted are of 1.98 and 6.82 mm at the vehicular load of 68 and 235 kN. The peak values of deflection have now been shifted at 3.6 m of subgrade length.

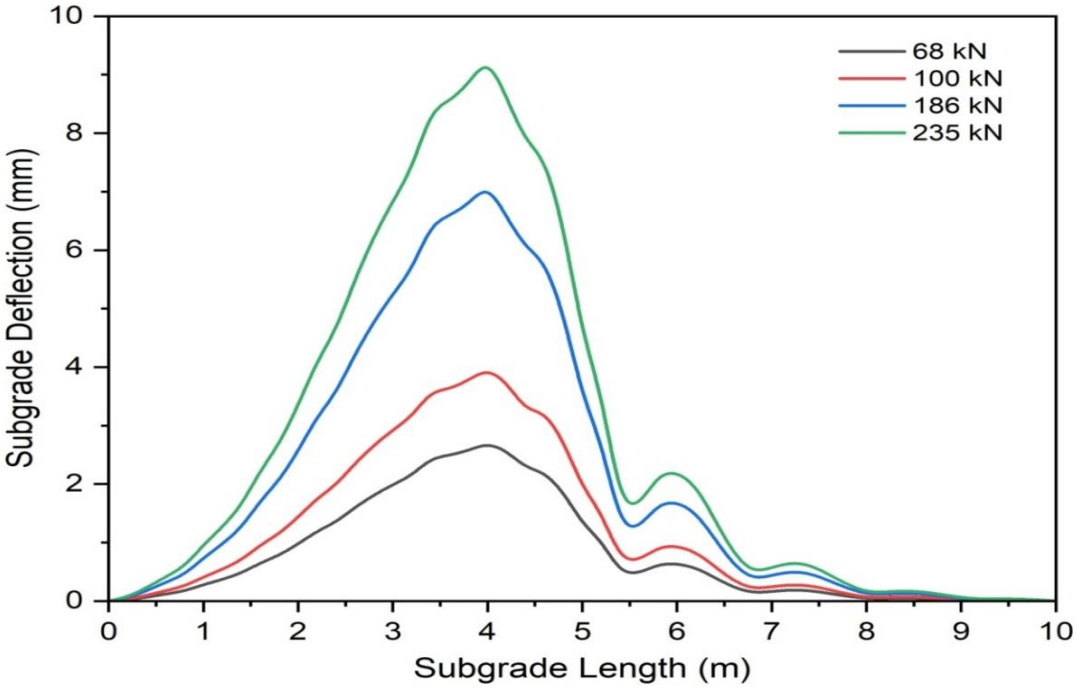

Figure 19: Response of unreinforced subgrade deflection at 25 m/s

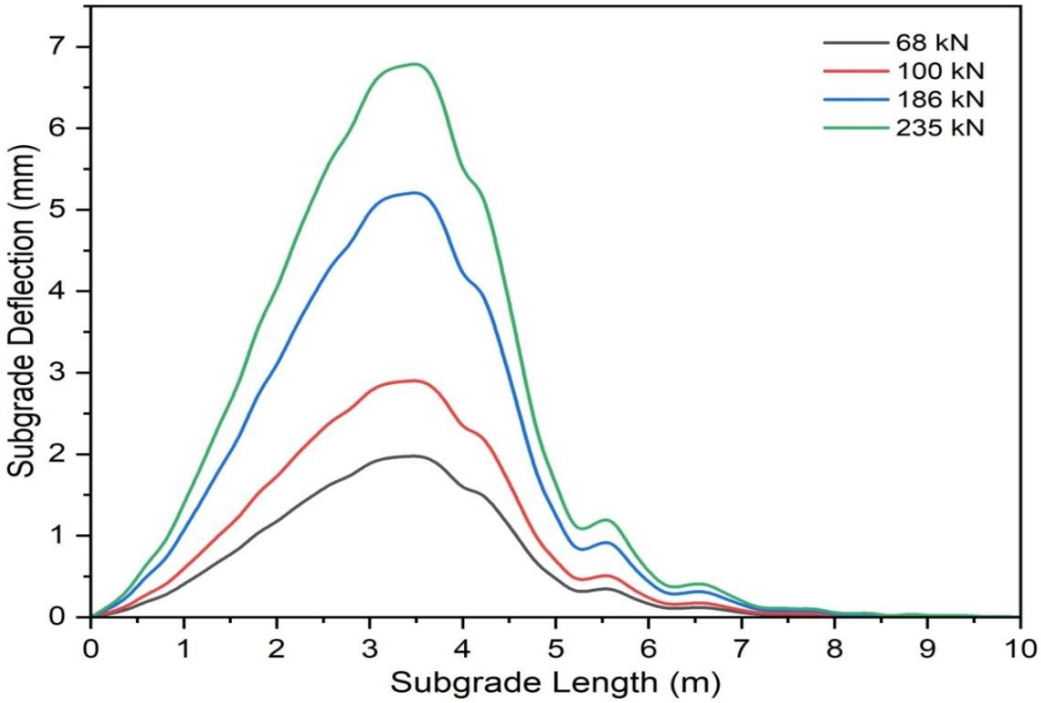

Figure 20: Response of unreinforced subgrade deflection at 30 m/s

The maximum deflection on the subgrade layer has been noted for variable vehicular velocity as shown in Table 5.

Table 5: Variation of maximum deflection with the velocity of vehicle

Velocity of Vehicle (m/s)	Subgrade Deflection (mm)			
	Single Axle with Single Wheel	Single Axle with Dual Wheel	Tandem Axle	Tridem Axle
10	1.9	2.8	4.97	6.83
15	3.07	4.51	8.1	10.55
20	3.03	4.46	8.01	10.44
25	2.7	3.97	7.13	9.3
30	1.98	2.91	5.23	6.82

Figure 21 showed the curve of load induced, velocity of moving vehicle vs. Maximum deflection of the subgrade layer. The velocity at which the interaction time of load and road layers starts to decrease is called as threshold velocity. The deflection on the subgrade has been seen increasing up to the threshold velocity; further the deflection has started decrease with increase the vehicular velocity. The threshold velocity for the subgrade layer has been seen at 20 m/s when the model is unreinforced with geogrid.

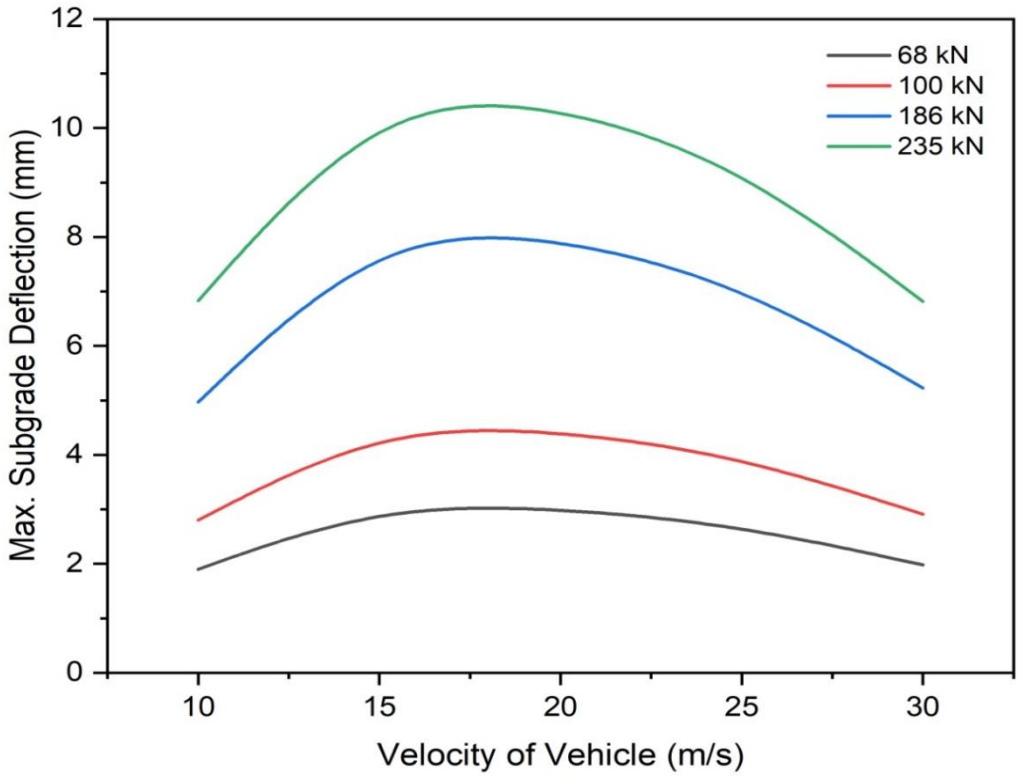

Figure 21: Variation of maximum subgrade deflection with vehicular velocity

The load – displacement curve has been plotted for the subgrade layer as shown in Figure 22. The maximum deflection of subgrade increases with increase in the loading intensity. But with variable vehicular velocity, the deflection increases initially up to the threshold velocity of subgrade then further decreases after the limit.

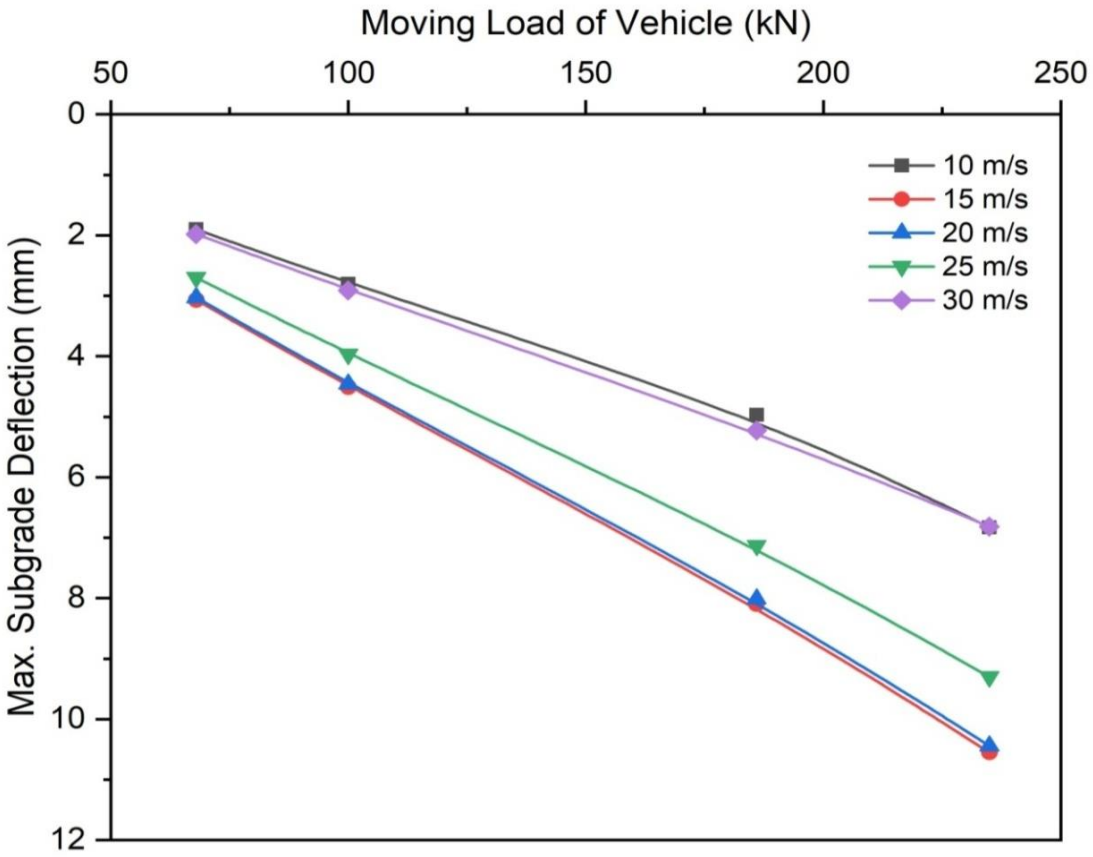

Figure 22: Variation of maximum subgrade deflection with moving load of the vehicle

Further, the road has been reinforced with two layer of geogrid. One has placed at the interface of base course – sub base course and other has been placed at the interface of Sub base course – Soft subgrade. After reinforcing the road model, the behaviour of soft subgrade is evaluated.

The displacement response of geogrid reinforced soft subgrade in the vertical direction at the velocity of 10 m/s has shown in the Figure 23. The minimum and maximum deflection that has been noted are of 0.81 and 2.82 mm which is reduced from the displacement value of 1.9 and 6.83 mm at the vehicular load of 68 and 235 kN respectively. The placement of geogrid also decreases the vertical vibrations in soft subgrade. The peak value of subgrade deflection can be seen at 5 m of pavement length.

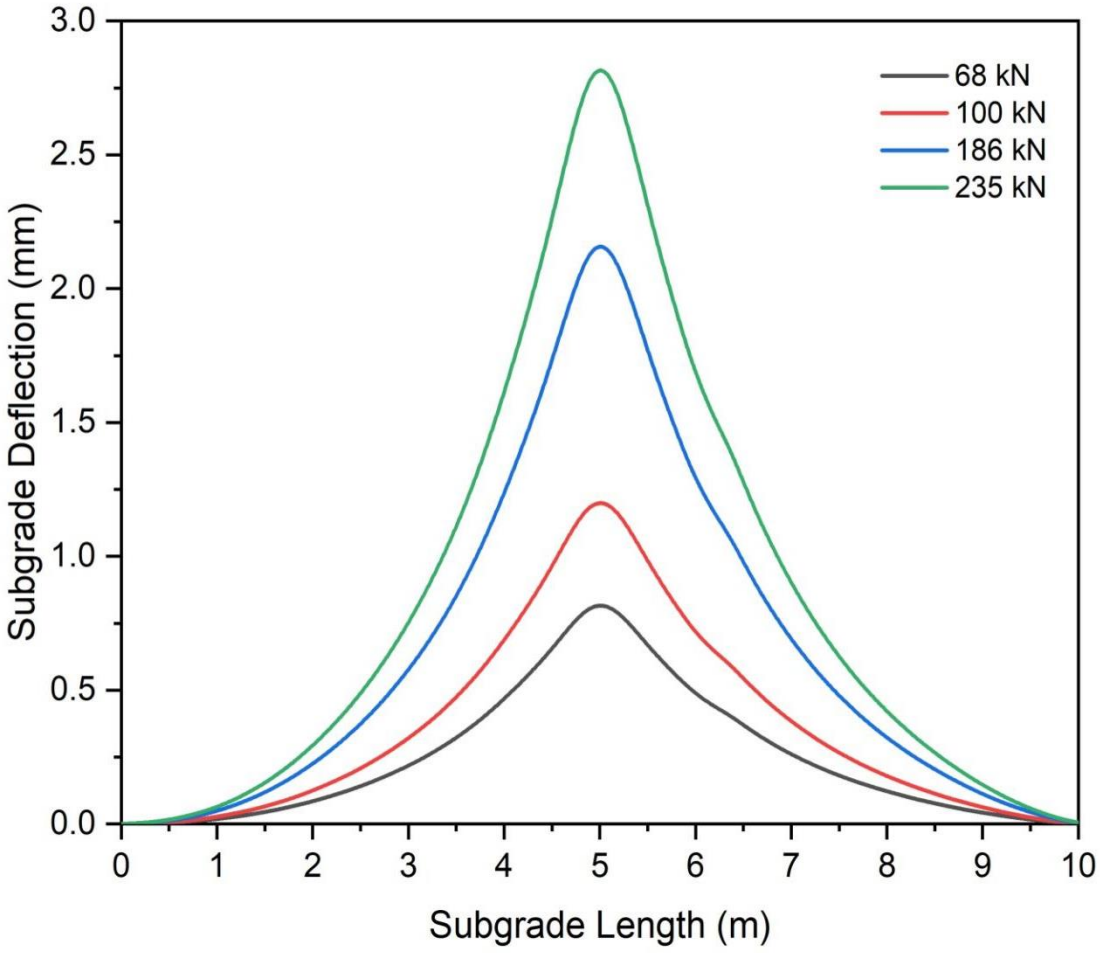

Figure 23: Response reinforced subgrade deflection at vehicular velocity of 10 m/s

Figure 24 shows the geogrid reinforced subgrade displacement response at vehicular velocity of 15 m/s. The minimum and maximum deflection that has been noted are 0.89 and 2.92 mm which has been reduced from 3.07 and 10.55 mm at the vehicular load of 68 and 235 kN. The peak value of the all the curves can also be seen at the 5 m of subgrade length.

Figure 25(a) shows the geogrid reinforced subgrade displacement response at vehicular velocity of 20 m/s. The minimum and maximum deflection that has been noted are of 1.10 and 3.82 mm which has been reduced from 3.03 and 10.44 mm at the vehicular load of 68 and 235 kN respectively. Figure 25(b) shows the boundary reflection in the displacement response of soft subgrade. It represent that the displacement has started to increase again instead to decreasing at the middle length of subgrade length when the vehicular load covered the 75% of road length.

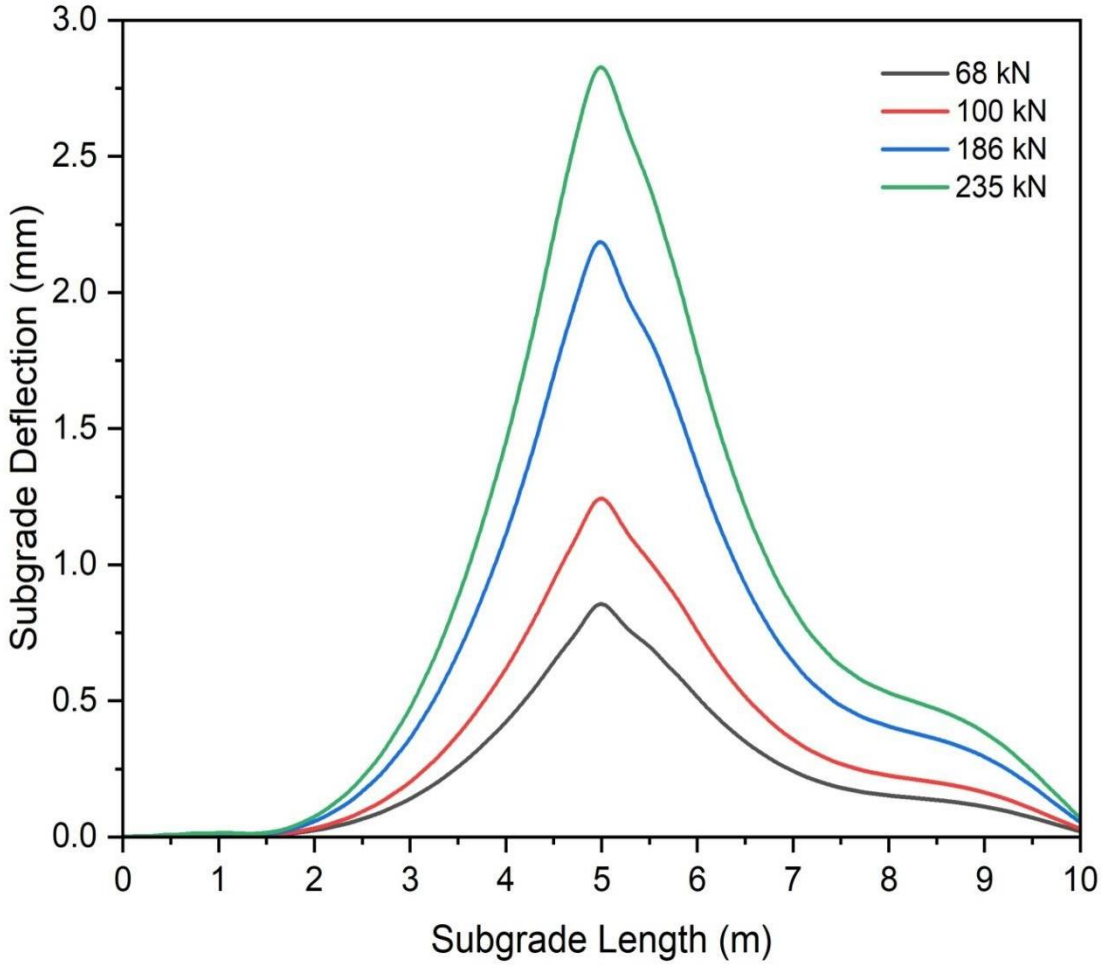

Figure 24: Response reinforced subgrade deflection at vehicular velocity of 15 m/s

Figure 26 shows the geogrid reinforced subgrade displacement response at 25 m/s of vehicular velocity. The minimum and maximum deflection that has been noted are of 1.36 and 4.71 mm which has been reduced from 2.7 and 9.3 mm at the vehicular load of 68 and 235 kN respectively. It has been observed that after the load crosses the reference node, the deflection of the soft subgrade has reduced rapidly at higher rate.

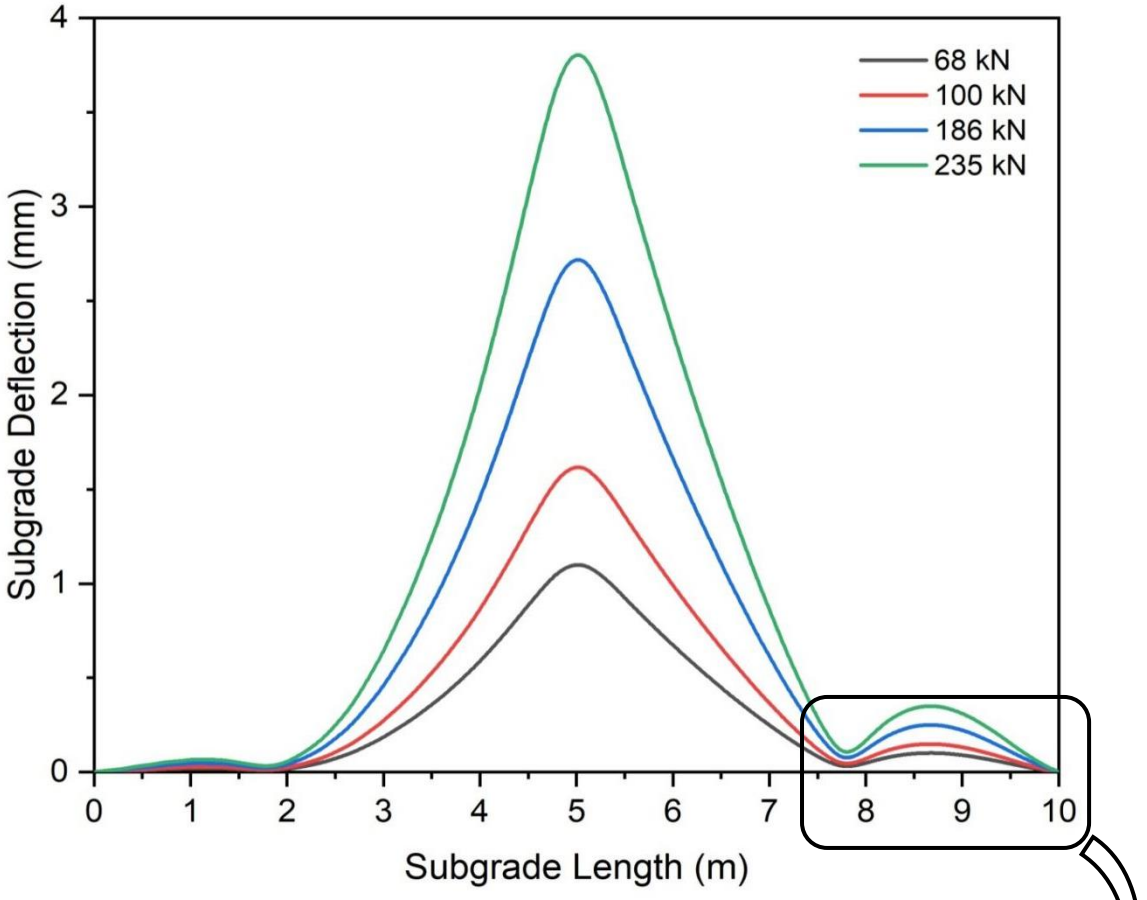

Figure 25(a)

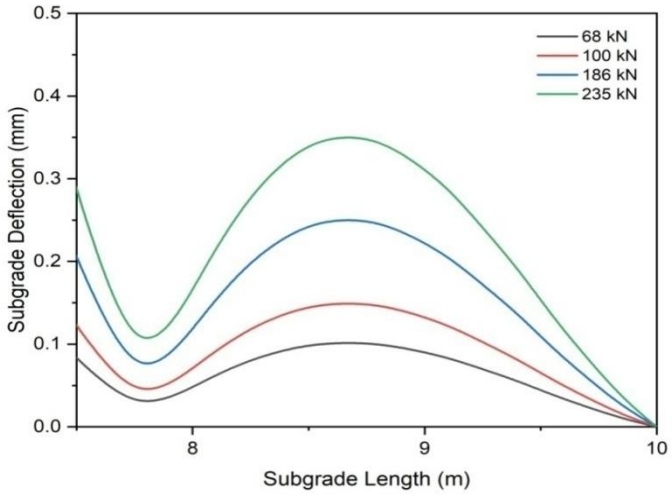

Figure 25(b)

Figure 25: (a) Response reinforced subgrade deflection at vehicular velocity of 20m/s **(b)** Boundary reflection on the subgrade

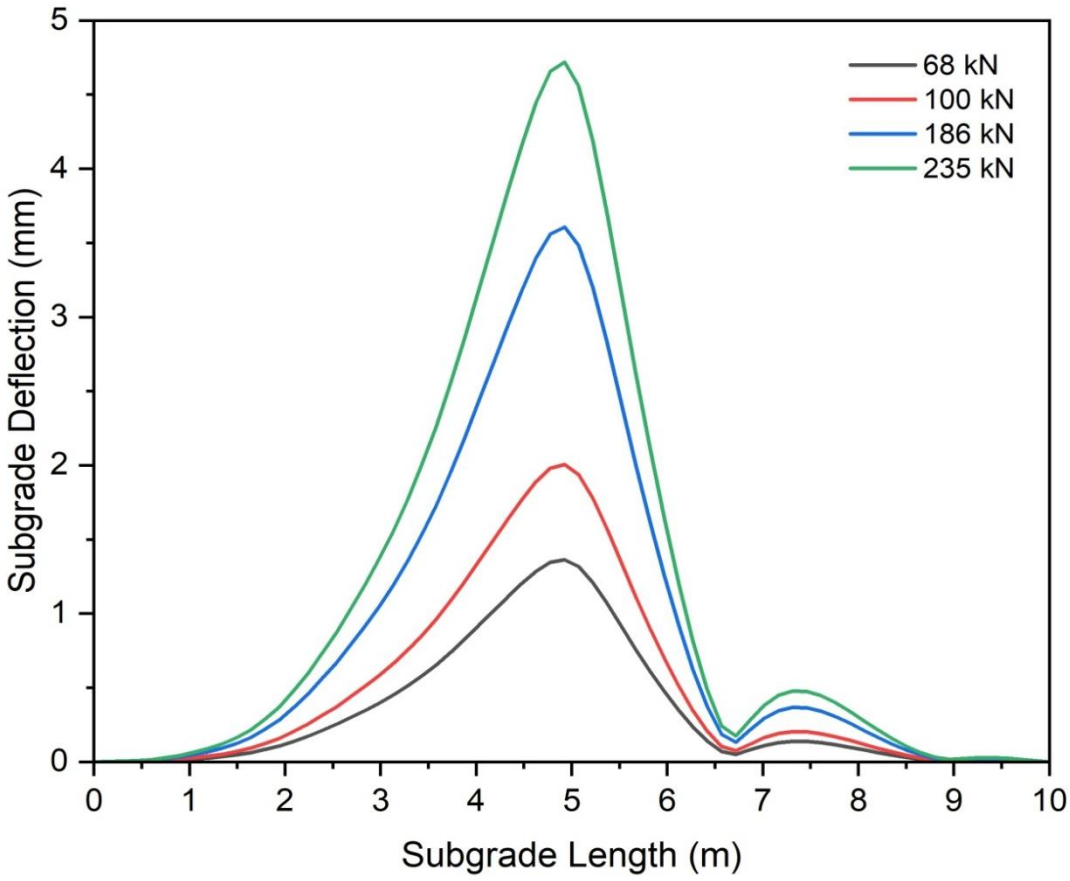

Figure 26: Response reinforced subgrade deflection at vehicular velocity of 25 m/s

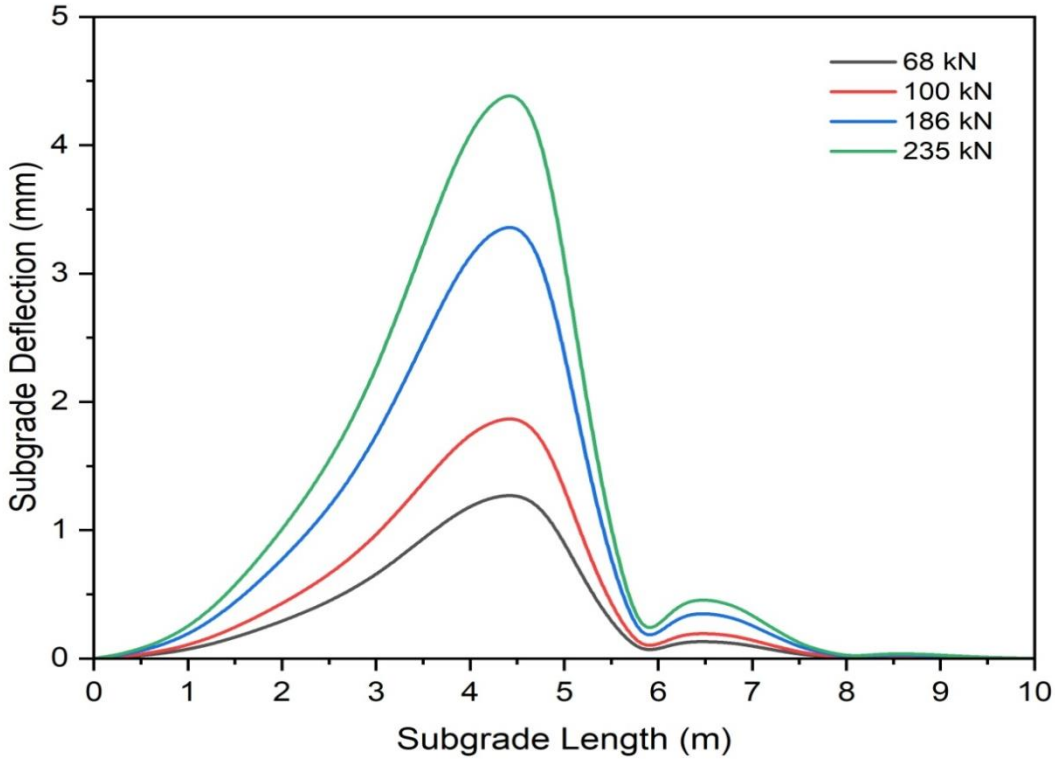

Figure 27: Response reinforced subgrade deflection at vehicular velocity of 30 m/s

Figure 27 shows the geogrid reinforced subgrade displacement response at 30 m/s of vehicular velocity. The minimum and maximum deflection that has been noted are of 1.27 and 4.39 mm which has been reduced from 1.98 and 6.82 mm at the vehicular load of 68 and 235 kN respectively. The peak value of the curves is shifted towards left side of reference point at 4.5 m of subgrade length. The interaction time between road and vehicular load started to reduce at 30 m/s velocity which reduces the deflection of the soft subgrade when compared to the previous reinforced subgrade results.

Table 6: Variation of maximum deflection of subgrade layer with the velocity of vehicle under unreinforced and reinforced unpaved road

Velocity of Vehicle (m/s)	**Section**	**Maximum Deflection of Subgrade (mm)**			
		Single Axle with Single Wheel	**Single Axle with Dual Wheel**	**Tandem Axle**	**Tridem Axle**
10	Unreinforced	1.9	2.8	4.97	6.83
	Reinforced	0.818	1.202	2.163	2.824
15	Unreinforced	3.07	4.51	8.1	10.55
	Reinforced	0.898	1.301	2.274	2.724
20	Unreinforced	3.03	4.46	8.01	10.44
	Reinforced	1.105	1.625	2.731	3.823
25	Unreinforced	2.7	3.97	7.13	9.3
	Reinforced	1.363	2.005	3.607	4.718
30	Unreinforced	1.98	2.91	5.23	6.82
	Reinforced	1.273	1.873	3.370	4.398

The maximum deflection on the geogrid reinforced subgrade layer has been noted for variable vehicular velocity as shown in Table 7.

Table 7: Variation of maximum deflection of stabilized subgrade layer with the velocity of vehicle

Velocity of Vehicle (m/s)	Subgrade Deflection (mm)			
	Single Axle with Single Wheel	Single Axle with Dual Wheel	Tandem Axle	Tridem Axle
10	0.818	1.202	2.163	2.824
15	0.898	1.301	2.274	2.724
20	1.105	1.625	2.731	3.823
25	1.363	2.005	3.607	4.718
30	1.273	1.873	3.370	4.398

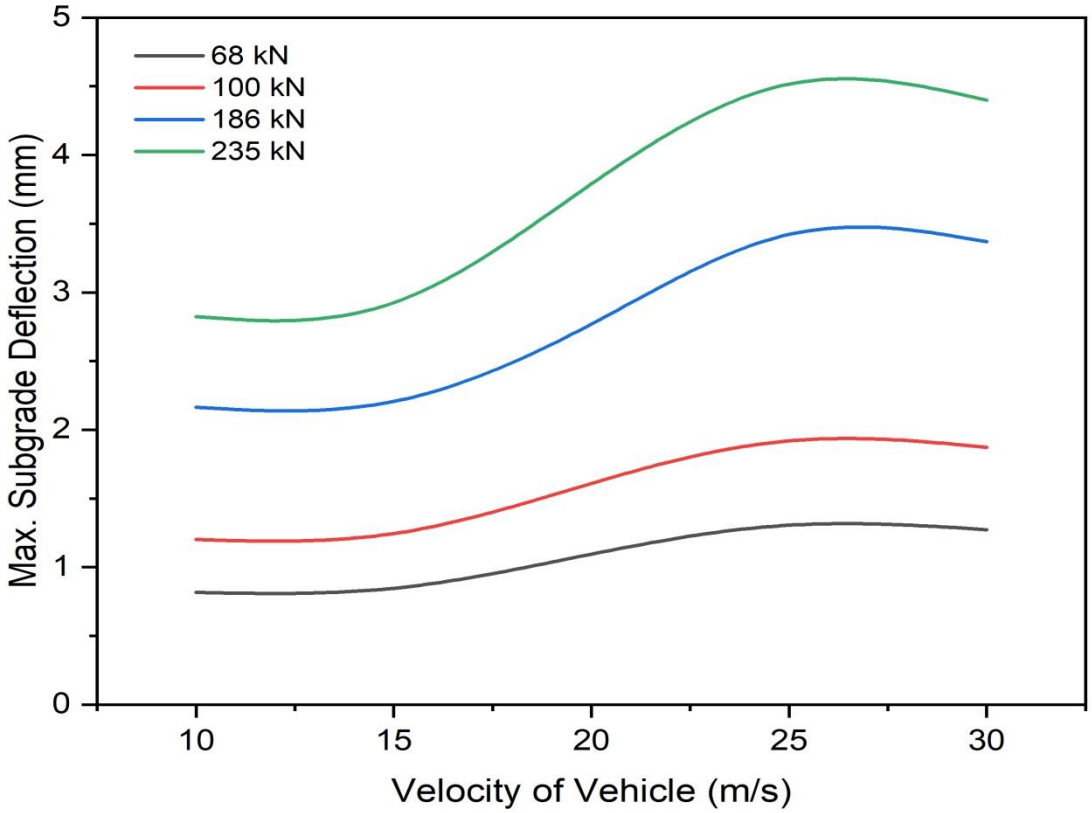

Figure 28: Variation of maximum reinforced subgrade deflection with vehicular velocity

Figure 28 showed the curve of loading induced, velocity of moving vehicle vs. Maximum deflection of the reinforced subgrade layer. The deflection on the reinforced subgrade has been seen increasing up to the threshold velocity; further the deflection has started decrease with increase the vehicular velocity. The threshold velocity for the

reinforced subgrade layer has been seen at 27 m/s when the model is reinforced with geogrid. The subgrade has stabilised by reinforcing with geogrid layer as the threshold velocity for the subgrade has increased from 20 to 27m/s.

The load – displacement curve has been plotted for the reinforced subgrade layer as shown in Figure 29. The maximum deflection of subgrade increases with increase in the loading intensity. But with variable vehicular velocity, the deflection increases initially up to the threshold velocity of subgrade (upto 25 m/s) then decreases further after the threshold limit.

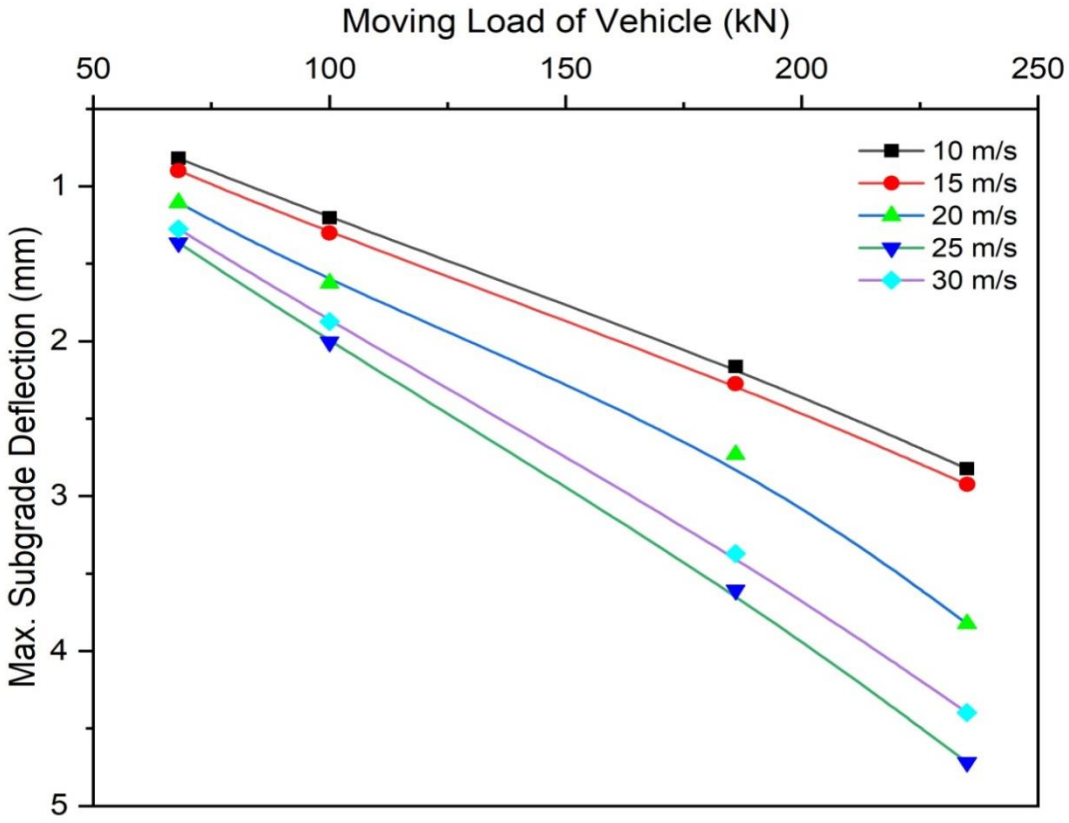

Figure 29: Variation of maximum reinforced subgrade deflection with moving load of vehicle

Efficiency of geogrid reinforcement with respect to the different vehicular velocities has shown in the Table 8.

Table 8: Efficiency of reinforced subgrade layer with variation in vehicular velocity

Velocity of Vehicle (m/s)	Efficiency of Subgrade Layer (%)			
	Single Axle with Single Wheel	Single Axle with Dual Wheel	Tandem Axle	Tridem Axle
10	54.95	57.04	56.46	58.64
15	74.27	74.27	74.22	74.17
20	63.52	63.56	65.90	63.37
25	49.48	49.48	49.40	49.26
30	35.66	35.63	35.56	35.51

The efficiency curve of geogrid reinforced subgrade layer with velocity of moving vehicle has shown in the Figure 30. The efficiency of the geogrid has increased for the

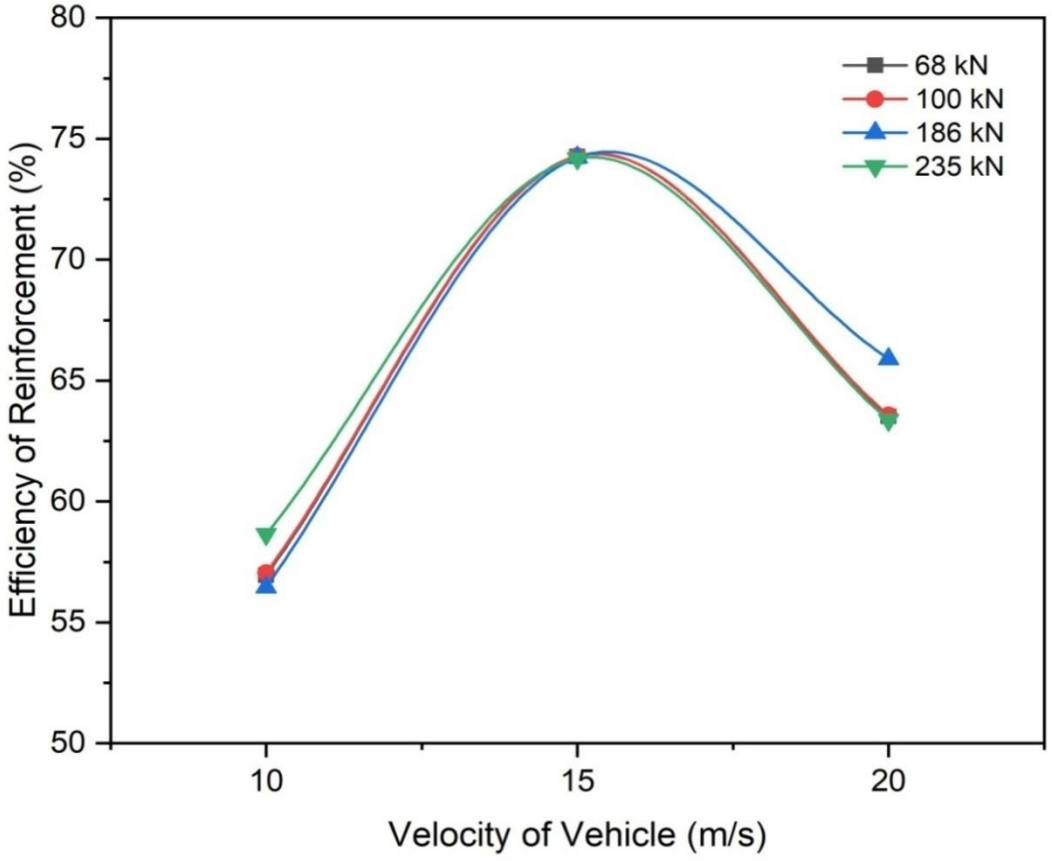

Figure 30: Efficiency of reinforced subgrade at variable vehicular velocities

vehicular velocity of 10 to 15m/s and then started to decrease for the further velocities. The maximum efficiency of geogrid layer has seen as 74.27% at vehicular velocity of 15 m/s. The behaviour of geogrid reinforced subgrade layer has seen to be similar for every loading intensity of moving vehicle.

4.2 DISCUSSION

The displacement response of the unreinforced and geogrid reinforced unpaved road model has been given in this study. For unreinforced unpaved roads, the deflection of the soft subgrade has been seen increasing with an increase in the intensity of moving load from 68 to 235 kN. But subgrade has shown dissimilar behaviour with the vehicular velocity. The deflection of the subgrade layer has seen an increase with an increase in vehicular velocity up to a specific limit called threshold velocity. The deflection has started to decrease with an increase in the vehicular velocity. The threshold velocity has been seen at 20 m/s for the unreinforced unpaved road.

Further, when the unpaved road stabilised with the geogrid layer, the comparison has done with the previous results of unreinforced unpaved roads. The deflection of the reinforced subgrade layer has been seen to be decreased as compared with the unreinforced unpaved road model. The behaviour of deflection has been seen as similar. The deflection has increased with an increase in the loading intensity of the vehicle. But again, it started to show different behaviour with the vehicular velocity. Initially, deflection increased up to the threshold velocity and then decreased with a further increase in the vehicular velocity. The threshold velocity for the stabilised subgrade has seen at the vehicular velocity of 27 m/s. The efficiency of the stabilised subgrade has also been calculated at variable vehicular velocity. The efficiency of the stabilised subgrade first increases with an increase in the velocity up to a specific limit which further decreases with an increase in the vehicular velocity. The efficiency of the stabilised subgrade has similar values with the variation of loading intensity of the vehicle. The maximum efficiency of the subgrade is 74.27% at a vehicular velocity of 15 m/s.

CHAPTER 5

CONCLUSIONS AND RECOMMENDATIONS

5.1 CONCLUSIONS

A finite element program has evaluated the dynamic response of unpaved roads subjected to moving vehicular load. The numerical model has been developed to study the central deflection in the soft subgrade. The results are compared among the unreinforced and geosynthetic reinforced unpaved road models. The effect of moving load on the soft subgrade has been reported in terms of deflection - velocity curve and velocity-dependent load-displacement curve. Further, the efficiency of the subgrade stabilized using geogrid has been evaluated. Based on the findings of this study, the following conclusions can be drawn:

- The deflection in the unreinforced and geogrid reinforced subgrade layer increases with an increase in the loading intensity of the moving vehicle.
- The deflection of the subgrade layer (in both cases) has increased with an increase in vehicular velocity up to a certain limit which is called threshold velocity. After reaching this limit, the deflection has decreased further with an increase in velocity.
- The peak of deflection curve has been shifted towards left side of middle length of the subgrade with increase in the vehicular velocity after reaching the threshold limit.
- The stabilization of the subgrade has also increased the threshold velocity of the vehicle from 20 m/s to 27 m/s.
- The geogrid reinforced unpaved road has reduced the vibrations caused by the moving vehicle.
- The behaviour of subgrade stabilized using geogrid shows consistent improvement in terms of efficiency for the set of selected loading parameters considered in the study. The maximum efficiency of the subgrade layer is 74.27% which has been seen at a vehicular velocity of 15 m/s.

5.2 RECOMMENDATION FOR FUTURE WORK

The results obtained from the modelling of unpaved road rested on soft subgrade are analysed for different loading and vehicular speed. Based on the work performed in the present study, the following recommendations for future work can be suggested.

- The study was performed on soft soil, which was clayey soil. By following a similar simulation technique, the results for different soil types can be found as this work has considered the single cycle, which can further be increased for future research. Experimental investigation can also be performed by using a number of layers for stabilization. Also, this work opens up a door to different new possibilities.
- These results can be utilized to calculate different parameters to estimate the settlement, bearing strength and shear strength of the soil.
- The study can also be extended to rigid pavements using the same techniques while changing the properties of road model.

References

1. Biabani, M.M., Indraratna, B. and Ngo, N.T., 2016. "Modelling of geocell-reinforced subballast subjected to cyclic loading." Geotextiles and Geomembranes, 44(4), 489-503.
2. Cao, Y.M., Xia, H. and Lombaert, G., 2010. "Solution of moving-load-induced soil vibrations based on the Betti–Rayleigh Dynamic Reciprocal Theorem." Soil Dynamics and Earthquake Engineering, 30(6), 470-480.
3. Chawla, S., & Shahu, J. T., 2021. "Analysis of cyclic deformation and post-cyclic strength of reinforced railway tracks on soft subgrade." Transportation Geotechnics, 28, 100535.
4. Chen, Y. H. and Huang, Y. H., 2000. "Dynamic stiffness of infinite Timoshenko beam on viscoelastic foundation in moving co-ordinate". Int. J. Num. Meth. Eng., 48, 1–18.
5. Fryba, L., 1987. "Dynamic interaction of vehicles with tracks and roads". Veh. Sys. Dy,.16, 129–138.
6. Fryba, L., 1999. "Vibration of solids and structures under moving loads". Thomas Telford Ltd., London.
7. Hardy, M. S. A., and Cebon, D., 1993. "Response of continuous pavements to moving dynamic loads". J. Eng. Mech., 119, 1762–1780.
8. Hardy, M. S. A., and Cebon, D., 1994. "Importance of speed and frequency in flexible pavement response". J. Eng. Mech., 120, 463–482.
9. IRC-37 (Indian Road Congress). 2018. Guidelines for the Design of Flexible Pavements. New Delhi.
10. IRC-58 (Indian Road Congress). 2015. Guidelines for the Design of Plain Jointed Rigid Pavements for Highways. New Delhi.
11. Keller, G.R., 2016. "Application of geosynthetics on low-volume roads". Transportation Geotechnics, 8, 119-131.
12. Kuleno, M. and Lera, E., 2020. Cause and Effects of Unpaved Road Deterioration-A Review.Global Scientific Journal: Volume 8, Issue 1.
13. Lahariya, A. and Trivedi, A., 2022. "Response Analysis of Multilayer Foundation System Supported by Soft Subgrade Subjected to Moving load". In Proc., International Conference of Structural Engineering and Construction Management (SECON-22).

14. Lahariya, A., Kumar, Y. and Trivedi, A., 2022. “Dynamic Analysis of Unpaved Roads Supported by Soft Subgrade Stabilised Using Geosynthetics”. In Proc., 4th Structural Integrity Conference and Exhibition (SICE-22).
15. Leshchinsky, B. and Ling, H.I., 2013. “Numerical modeling of behavior of railway ballasted structure with geocell confinement”. Geotextiles and Geomembranes. 36. 33-43.
16. Mamlouk, M. S., 1997. “General outlook of pavement and vehicle dynamics”. J. Trans. Eng., 123(6), 515–517.
17. Mehra, S., and Trivedi, A., 2021. “Pile Groups Subjected to Axial and Torsional Loads in Flow-Controlled Geomaterial.” Int. J. Geomech., 21(3), 1-15.
18. Ngo, N.T., Indraratna, B., Rujikiatkamjorn, C. and Mahdi Biabani, M., 2016. “Experimental and discrete element modeling of geocell-stabilized subballast subjected to cyclic loading.” Journal of Geotechnical and Geoenvironmental Engineering, 142(4), p.04015100
19. Peketi, G., 2019. “Usage of Geogrids in Flexible Pavement Design.” International Journal of Engineering Sciences and Research Technology. 22. 10. 10.5281/zenodo.1215426.
20. Satyal, S.R., Leshchinsky, B., Han, J. and Neupane, M., 2018. “Use of cellular confinement for improved railway performance on soft subgrades.” Geotextiles and Geomembranes. 46(2). 190-205.
21. Singh, M.; Trivedi, A.; Shukla, S., 2020. “Unpaved test sections reinforced with geotextile and geogrid”. Materials Today: Proceedings. 32. 10.1016/j.matpr.2020.03.260.
22. Singh, M., Trivedi, A. and Shukla, S.K., 2022. “Evaluation of geosynthetic reinforcement in unpaved road using moving wheel load test.” Geotextiles and Geomembranes.
23. Sun, L. and Luo, F., 2007. “Arrays of dynamic circular loads moving on an infinite plate”. Int. J. Num. Meth. Eng., 71, 652–677.
24. Tang, C., Lu, Z., Duan, Y. and Yao, H., 2020. “Dynamic responses of the pavement-unsaturated poroelastic ground system to a moving traffic load”. Trans. Geotech., 25, 1-8.
25. Theuns, H., Peter, K. and Christopher, R., 2006. “Surfacing Alternatives for Unsealed Rural Roads,” in Transport Note No. TRN-33, Washington, DC.

26. Trivedi, A., and Singh, S., 2004. “Cone Resistance of Compacted Ash Fill.” Journal of Testing and Evaluation. 32. 429-437. 10.1520/JTE11906.
27. Wu, C.P. and Shen, P.A., 1996. “Dynamic analysis of concrete pavements subjected to moving loads.” Journal of transportation engineering, 122(5), 367-373.
28. Zafir, Z., Siddharthan, R., and Sebaaly, P. E., 1994. “Dynamic pavement–strain histories from moving traffic load”. J. Trans. Eng., 120(8), 21–42.